TÉCNICO LISBOA

Multi-azimuth Seismic Inversion Workflow Optimization for Anisotropy Estimation

João Pedro Pereira de Almeida

Thesis to obtain the Master of Science Degree in

Petroleum Engineering

Supervisor(s): Prof. Leonardo Azevedo Guerra Raposo Pereira
Msc Romain Pierre Baillet

Examination Committee

Chairperson: Prof. Maria João Correia Colunas Pereira
Supervisor: Msc Romain Pierre Baillet
Member of the Committee: PhD. Hugo Manuel Vieira Caetano

January 2021

Declaration

I declare that this document is an original work of my own authorship and that it fulfills all the requirements of the Code of Conduct and Good Practices of the Universidade de Lisboa.

Acknowledgments

First of all I want to thank Beicip-Franlab for the opportunity to do this work and all the care I received during my five months in Paris. My thanks to the entire team who always made me feel comfortable and welcome, especially to Romain for guiding and teaching me during the internship. I also want to thank the Portuguese unknown man who clean the office at the end of the day, for reminding me of home.

I want to thank professor Leonardo for providing me with this opportunity and for the patience to correct and guide me into always producing a better work.

I also want to thank my friends from *Cardápio* and from Leiria for the all memories we shared. Hopefully we can all be together soon.

Next, I want to thank Sofia, this adventure would have been very different without you.

Finally, I want to thank my family for always being there in every step of my life. They know how much they mean to me. I want to give especial thanks to my cousin, André, who received me with open arms in Paris and helped me to adapt to a different country.

Resumo

A boa qualidade de imagens sísmicas é crucial nas fases de exploração e produção de um reservatório de hidrocarbonetos. Boa qualidade da sísmica permite o desenvolvimento de modelos de reservatórios com maior precisão e qualidade. A capacidade de fazer aquisições sísmicas com uma boa cobertura azimutal pode ser valioso para a estimação de anisotropia, o que resulta numa melhor identificação do sistema de fraturas.

Este estudo propõe uma melhoria em inversões deterministicas baseadas em modelos assente numa metodologia para dados sísmicos multi-azimutais já existente. Uma nova metodologia para a wavelet é proposta, que usa apenas uma única wavelet para todos os sectores azimutais em vez de diferentes wavelets por sector. Esta modificação procura reduzir qualquer anisotropia artificial induzida pelo uso de diferentes wavelets e assim produzir resultados mais precisos. Este estudo também procura otimizar os parâmetros de inversão de sísmica multi-azimutal, promovendo assim a caracterização e quantificação da anisotropia presente nos dados sísmicos.

Esta tese centra-se em volta de dois tipos de inversão determinística (*sequential* e *joint*) especificas de dados sísmicos multi-azimutais e como estes podem ser utilizados na quantificação de anisotropia. Diversas otimizações aos parâmetros a usar por estas inversões foram realizadas de modo aos resultados de ambas serem idênticos, o que é necessário na análise anisotrópica. Esta análise (anisotrópica) é o elemento chave da tese uma vez que o propósito de usar dados sísmicos multi-azimutais é detetar e caracterizar anomalias anisotrópicas. Nesta tese vai ser desenvolvido todo o processo de inversão sísmica multi-azimutal e os resultados serão interpretados em relação à origem da anisotropia existente.

Palavras-chave: Inversão sísmica, inversão azimutal, anisotropia sísmica

Abstract

The quality of seismic images is crucial in the exploration and production stages of a hydrocarbon reservoir. Good seismic quality can lead to the development of reservoir models with a more accurate target description. The ability to perform seismic acquisitions with a good azimuthal coverage can be valuable for anisotropy estimation leading to better fracture and overall system characterization.

This study proposes to improve a deterministic model-based seismic inversion workflow building upon multi-azimuth seismic data workflow already existent. A new wavelet use is proposed, using a single wavelet for all azimuthal sectors instead of different wavelets per sector. This modification seeks to reduce the artificial anisotropy induced by the minimal differences between wavelets of different amplitudes, leading to a more accurate result. The study also deals with the optimization of the multi-azimuth seismic inversion parameters, promoting the characterization and quantification of the anisotropy present in the dataset.

This thesis is centered around two types of deterministic inversions (sequential and joint), specific to azimuthal data, and how they can be used in anisotropy quantification. Several optimizations are performed to the parameters used by the sequential and joint inversions so that both can produce similar results which are needed for the anisotropy analysis. The anisotropic analysis is the key element of the thesis, the objective of using multi-azimuth seismic data is to detect anisotropic anomalies and characterize them. The thesis will develop the workflow for multi-azimuth seismic data inversion and will interpret the data regarding the origin of the existing anisotropy.

Keywords: Seismic inversion, azimuthal inversion, seismic anisotropy

Contents

List of Acronyms

CDP – Common Depth Point

HTI - Horizontal Transverse Isotropy

ISD – Impedance Standard Deviation

MAZ – Multi-Azimuth

MCA – Multi-trace Coherency Analysis

NAZ – Narrow-Azimuth

NMO – Normal Moveout

ppg – Pounds per gallon

RAZ – Rich-Azimuth

SSI – Sparse-Spike Inversion

TI – Transverse Isotropy

VTI – Vertical Transverse Isotropy

WAZ – Wide-Azimuth

List of Figures

Chapter 1

Introduction

1.1 Motivation

The Oil and Gas industry has a footprint present in every corner of the world. Its role in the energy market, economy, politics, development is undisputedly high. Like any industry, is subject to new challenges, and so, factors like efficiency, cost optimization and environment have been increasingly important to drive the industry further [1][2].

In a competitive world, the search for the best results is essential to secure business opportunities. Decisions need to be accurate, and so needs to be the knowledge behind it. The oil and gas upstream stages based on seismic amplitude analysis are fundamental in the decision making. Knowledge provided by seismic inversion is fundamental in the exploration and production of hydrocarbons, through it is possible to create models of the subsurface of the earth and identify geological formations prone to hydrocarbon accumulation. Naturally, significant developments are being made in the way that seismic data is applied in the industry, especially in the use of 3D seismic to identify geological structures and to predict reservoir properties accurately to avoid missing exploration opportunities [3].

Conventional 3D seismic surveys use a single line of orientation, this is, narrow-azimuth (NAZ), which results in illuminating only one shooting direction. However, for complex geological areas something more is necessary. When coherent noise is too complicated to be interpreted and the reservoir illumination is irregular or discontinuous, different approaches are necessary to answer these problems and ensure that the best possible decision is made to avoid expensive failures. These difficulties drove the development of more complete survey strategies to achieve better reservoir identification such as multi-azimuth (MAZ), wide-azimuth (WAZ) and rich-azimuth (RAZ) surveys which started to be widely used on more challenging areas [4].

Acquiring seismic data using MAZ surveys and performing deterministic model-based inversions can be a useful tool to identify seismic anisotropy and better characterize fracture parameters with origin in azimuthal P-wave data that otherwise would be left unnoticed. If the results are satisfactory, a more accurate analysis of the system is possible, thus, maximizing the confidence in the created model of the subsurface.

This thesis results in the work performed during an internship at Beicip-Franlab, an international oil and gas consulting and software provider. The work explores the MAZ seismic inversion module of InterWell®, the seismic inversion and characterization software for reservoir and exploration geophysicists developed by Beicip-Franlab.

1.2 Objectives

This thesis aims at using the MAZ deterministic model-based inversion to obtain precise information regarding the origin of the seismic anisotropy, which can be very important when performing a fracture characterization of the subsurface.

The procedure to be implemented seeks to explore and optimize the MAZ inversion module of InterWell® (Beicip-Franlab) by providing new solutions, such as a new wavelet methodology and the inversion parameter optimization, to the current workflow. Using the enhanced workflow the author will interpret the anisotropic anomalies present in the data giving an explanation regarding its origin.

1.3 Structure of the thesis

The thesis is introduced with the motivation and objectives proposed in the first chapter. In the second chapter the seismic inversion related concepts in use will be introduced, including the more specific inversion by azimuth.

In the third chapter the methodology applied will be presented, focusing in the several steps necessary to successfully accomplish the proposed objective. Of special importance in this chapter is the concept of Joint inversion and Sequential inversion, two inversion sub-types specific to the azimuthal inversion module.

The fourth chapter is where the application of the methodology is presented and the results discussed. The geological framework is also included in this chapter along an extensive parameter optimization of the inversion process. After the parameter optimization the main results are presented combining every available information to quantify the origin of the anisotropy in the studied area. Also secondary results outside the major focus of the thesis are exposed in this chapter. Here is included an interesting alternative to enhance the computational performance of the inversion and the final observations regarding the impact of the new wavelet methodology in the project. The chapter closes with a discussion of the obtained results.

The fifth and final chapter concludes the thesis, a final overview of the subject is presented with a note to the future work to be developed.

Chapter 2

Theoretical background

This chapter purpose is to introduce the theoretical concepts needed in the thesis. The focus is the seismic inversion methodologies with more depth to the deterministic and how it connects with azimuthal acquisition. Finally, a simple introductory notion of seismic anisotropy and the theory behind the wavelet is given.

2.1 Seismic inversion

Geophysical methods study the propagation of physical fields inside the earth, measuring its response to determine and describe complex geological structures. The earth´s measured feedback which describe the physical system is determined by the rock properties. This knowledge allows geophysicists to make predictions and create subsurface models. To build these subsurface geological models different approaches can be used. The laws of physics provide the means to compute measurements given a model, this is called a *forward problem*. It is also possible to use the results of some measurements to predict the values of the parameters that characterize the system, explaining the observed data while taking uncertainty into consideration, this is called the *inverse problem* [5].

While forward problems allow, considering an earth model, to predict the values of seismic signals, for other geophysical applications, such as seismic inversion, the opposite is needed, this is, to create a model of the earth given measured signals at a specific location [6]. Seismic inversion can be briefly defined as a technique for creating a model of the earth from observed data. As the name hints, seismic inversion, being an inverse problem, directly opposes the forward approach [7]. The main goal when using seismic inversion methods is to predict reservoir properties and characterize rock properties such as lithology, porosity, fluid content as well as the conditions to which they are subjected, like pressure and temperature [8]. The seismic data inversion presents practical challenges, for instance, noise being always present in the data, forward modeling simplifications need to acquire solutions in reasonable time, uncertainties when estimation a wavelet and difficulties when associating reservoir and elastic properties [8].

To understand seismic inversion, one must first comprehend forward modeling and the convolutional model, as it is a centerpiece to the inversion process. The convolutional model is a simple common method to model a seismic trace. Seismic reflections occur in the presence of contrast in elastic properties across the different layer interfaces from which is possible to calculate the reflection coefficient for each reflecting interface. The earth reflectivity is an impulse response with amplitudes matching the reflection coefficient for each subsurface layer. The convolution is simply the earth's reflectivity *r(t)* convolved with source wavelet *w(t)* resulting in the seismic trace *s(t)* (Equation 2.1) [9]. When the noise *n(t)* component is considered, the convolutional model can be written taking it into consideration (Equation 2.2) [7]. While in forward modeling the unknown parameter is the seismic trace and therefore the convolution is used, for seismic inversion the objective will be to calculate the earth's reflectivity (knowing the seismic trace) and to do so an inverse process must be applied, this is called deconvolution.

$$s(t) = w(t) * r(t) \tag{2.1}$$

$$s(t) = w(t) * r(t) + n(t) \tag{2.2}$$

2.2 Deterministic seismic inversion

In general there are two main groups for seismic inversion methods, the deterministic and the stochastic [8][3]. Deterministic inversions consist in the minimization of the difference between a modeled seismic trace and the actual trace, and are therefore based on optimization algorithms that aim for a single best fit solution [10][8][3]. Additional terms are usually included in the objective function to condition the solution into fitting a specific criteria [8]. Within stochastic inversions geostatistical inversions are based on geostatistical simulations to generate diverse realizations at reservoir model scale. Each realization can be matched to the seismic trace, honoring the statistics of property variation between points and teeing the wells precisely. These realizations can be turned into reservoir properties and analyzed in terms of uncertainty as well as connectivity [3].

The deterministic approach presents some limitations. It only represents the best estimations within the limitations of the data bandwidth meaning the uncertainty assessment is limited to the best fit solution [10][3]. The geostatistical methods can address the deterministic issues better however tend to be more computationally demanding, time consuming and therefore expensive when comparing with deterministic methodologies [8][3].

There are several deterministic methods, being the most commonly used the sparse-spike techniques and model-based inversions [8]. Sparse-Spike Inversion (SSI) consists in a group of techniques where the seismic trace can be modeled with reduced, but large, reflection coefficients (spikes). This assumes that the underlying elastic properties are sparse. Basically, a sparse-spike series is broadband, this is, attempts to recover a spiky reflectivity from band-limited seismic data. The objective is to get a high-resolution impedance profile from band-limited seismic data that correlates the formation lithology [11][7][3]. The advantage of the SSI is the consistency with the seismic data presented by the model since it creates changes in elastic properties only when necessary to match the seismic response. Can be considered a oversimplified model of the subsurface [3]. Even though the similarities, SSI techniques can vary greatly, especially in the way the sparsity is computed, how the constraints are defined, how the L1 (sparsity) and L2 (match with the seismic) norms are utilized and how the local minima are avoided [11].

Model-based inversions are a popular inversion technique for commercial software [3]. In this type of inversions there is an initial impedance model that provides the low frequency component not present in the seismic bandwidth. The model is convolved with the wavelet to obtain a response which is compared with the seismic and constantly updated until the seismic response fits the seismic data upon some determined criteria where the errors are minimized, as demonstrated in Figure 2.1 [11][7][3]. The starting model can be an interpolation of well data or a trend model based on geological knowledge [3]. This is an appealing method since it avoids the direct inversion of the seismic data itself, however, at the same time is possible to obtain a model that matches the seismic data perfectly but is incorrect [7].

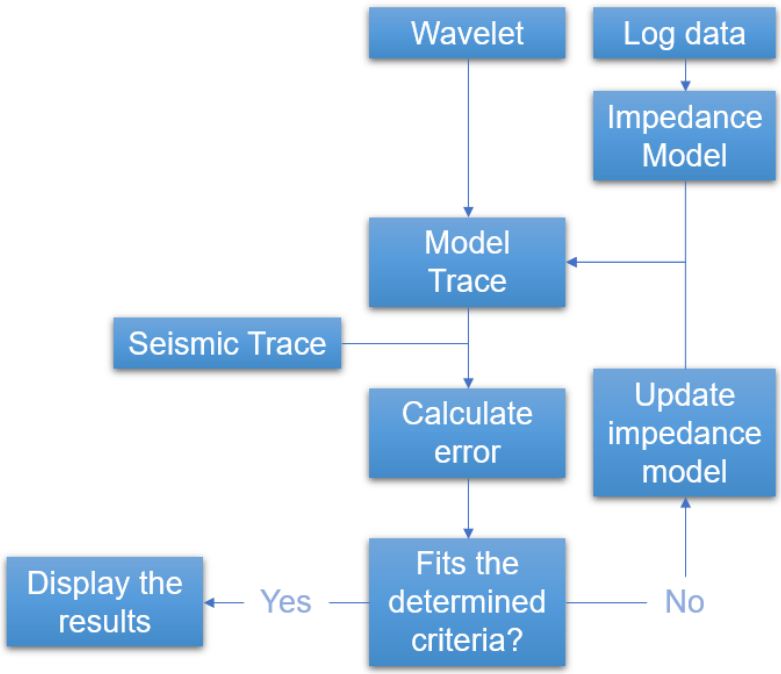

Figure 2.1: Generalized diagram for Model-based inversions adapted from [3].

2.3 Azimuthal seismic acquisition

Achieve acceptable mapping of the subsurface properties is a challenging process, therefore, alternative acquisition methods dedicated to successfully illuminate and create 3D models of the most complex geological structures are needed. For this purpose, seismic acquisition techniques have been developed, using not only gathers by offset, but also by azimuth.

There are several methodologies for azimuthal acquisition, such as NAZ, MAZ and WAZ [12][4][13]. Conventional 3D marine surveys are acquired using a long and narrow spread of streamers that are towed by one ship (in marine acquisition) resulting to sources and receivers having a relatively common azimuth causing the subsurface to be mapped in that shooting direction. This is the case for the NAZ survey, represented in Figure 2.2. This type of acquisition assumes that the target to map is fairly uniform which allows to create clean seismic images capable of accomplishing the proposed exploration and appraisal objectives. However, when the target is too complex, and the coherent noise is too complicated thus preventing the interpretation of the subsurface, other techniques could be used [4]. This is the case for MAZ and WAZ. MAZ methodology is the combination of several NAZ surveys on the same target but from different shooting directions providing a better-quality target illumination, as represented in Figure 2.2 [4][13]. WAZ surveys are similar to NAZ with the difference of offering a much wider azimuthal angle. This is achieved by using a higher aspect ratio (i.e. crossline dimension of the patch divided by the inline dimension) of the recording patch. Aspect ratios until 0.5 are considered NAZ, while greater than 0.5 are considered WAZ [12]. In a marine acquisition the WAZ survey is performed usually by adding one or more source vessels [13]. Narrow, multi and wide azimuthal acquisitions represent just some of the possible methods for azimuthal survey, for instance, combining MAZ and WAZ techniques result in another called RAZ [4].

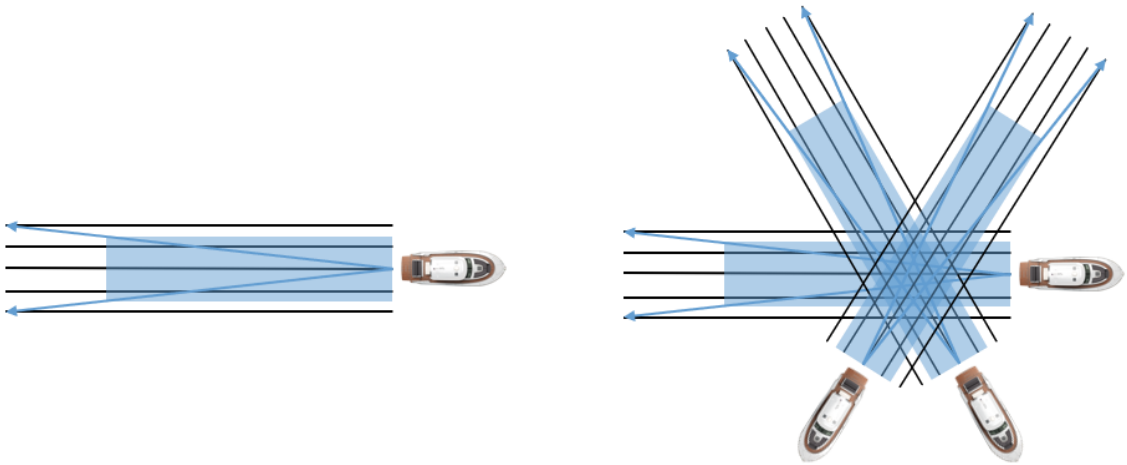

Figure 2.2: Representation of NAZ seismic marine acquisition on the left. Representation of MAZ seismic marine acquisition on the right.

2.4 Seismic anisotropy

Anisotropy is defined as the *"variation of a physical property depending on the direction in which it is measured"* [14]. Seismic anisotropy can therefore be defined as a *"directional variation of a material's response to the passage of seismic (elastic) waves"* [15]. The role of anisotropy has rapidly increase in the past two decades and is important in geophysics due to its inevitable impact on seismic data [15].

The most common anisotropy model is transverse isotropy (TI). In materials following this anisotropic model there is only one rotational symmetry axis, and so, in directions perpendicular to that same axis, the material properties appear to be directionally invariant. When the symmetry axis is vertical it is called vertical transverse isotropy (VTI), when it is horizontal is called horizontal transverse isotropy (HTI) [16][15] (Figure 2.3). Anisotropy is interesting to consider mainly for two purposes, firstly to improve seismic images by considering VTI as anisotropy during the processing of the seismic data, attribute analysis and interpretation and secondly to extract fracture information from seismic data [15].

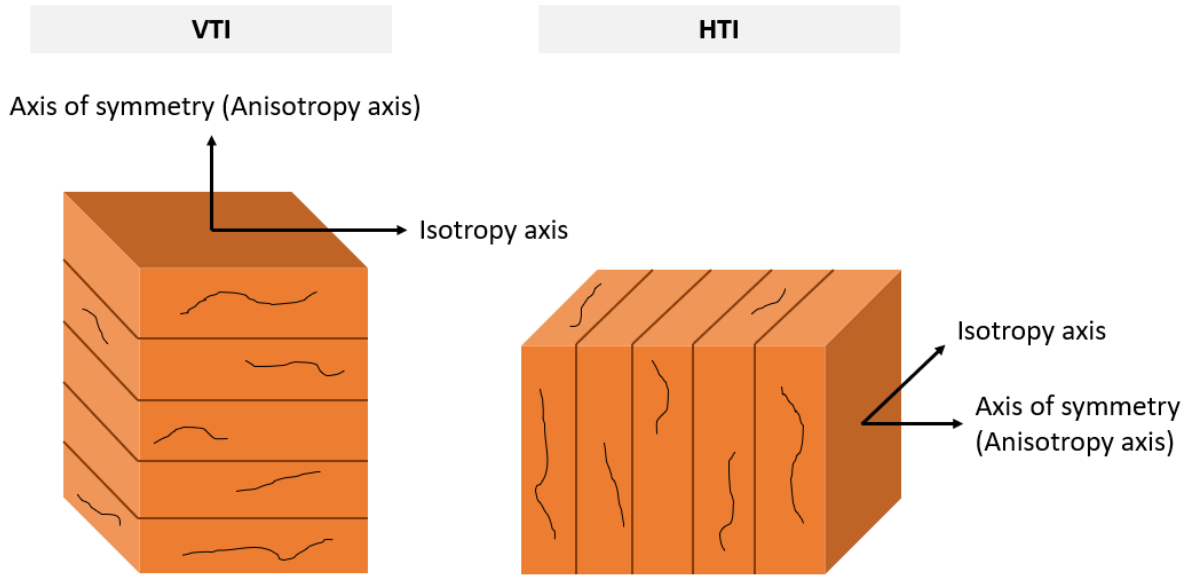

Figure 2.3: Transverse isotropy (TI) is the most commonly used anisotropy model in applied geophysics [15]. When the symmetry axis of a TI media is vertical, it is called vertical transverse isotropy or VTI (left). When the symmetry axis is horizontal, it is called horizontal transverse isotropy or HTI (right).

Multi-azimuth seismic can be used to achieve sub-seismic lateral resolution. Even though many individual fractures are smaller than the seismic resolution and cannot be directly observed it is possible to obtain a response from several fractures trending in a determined direction. This leads to a directional dependence where velocities are azimuthally anisotropic, thus, enabling the use of seismic anisotropy to fill the gaps between the characterization of microscopic and macroscopic fractures [15]. The concept of azimuthal anisotropy refers to a given property, for instance amplitude, that varies with azimuth reflecting the existence of anisotropy [16][17].

2.5 Wavelet theory

As previously said, the objective when using seismic inversion methods is to infer reservoir properties by constructing models of the subsurface. However, to achieve this goal its necessary to connect the seismic data to the geology. The seismic wavelet is the tool that serves as link between these parameters and must be known to perform a correct geological interpretation making it an essential component of any seismic inversion. Even though seismic data can provide a good image of the subsurface, without the wavelet there are several equally valid possible interpretations for the geology. When acquiring seismic data, the subsurface is mapped using a field wavelet, which is reflected from rock layers and recorded at the surface as a raw field trace. At lithologic borders the reflection coefficient in rock properties determines how much of the wavelet's energy is reflected to the surface. The deconvolution is the procedure used to convert the field wavelet to the desired broad band-zero phase wavelet [18][3].

A wavelet, in a basic way, represent an anytime varying signal into its frequency and time component simultaneously. The seismic signal is an impulsive pulse which decays over time, however, using mathematical models is possible to decompose that signal into a series of periodic functions which, in general, have amplitude and phase that vary with the frequency. The variation of the amplitude of waves with the frequency is represented by the amplitude spectrum while the range of frequencies above a determined threshold is normally described as the bandwidth of the wavelet [3].

To define the shape of the wavelet its necessary to calculate its amplitude spectrum and phase. The amplitude spectrum can be estimated from the seismic trace using, for instance, a Fourier Transform (deconvolution) of the seismic, while the phase is the shift of the waves at each frequency [3]. In most of the cases, seismic data is processed assuming a minimum phase wavelet (from explosive sources and airguns with no energy before zero followed by a quick increase), however, most field phases are not, and using minimum phase deconvolutions often results in mixed-phase wavelets instead of the desired zero-phase (where the peak frequencies are aligned to zero). By converting the mixed-phase wavelet to zero-phase or simply by knowing its effects is possible to use it when creating a model of the subsurface [18][3].

Chapter 3

Methodology

This chapter addresses the methodology applied in this thesis. To achieve the proposed objectives, its necessary to go through InterWell® (Beicip-Franlab) key steps. The azimuthal inversion module of the software was designed to take advantage of the MAZ seismic acquisition to highlight possible impedance anomalies that otherwise would be very hard to detect.

Four important stages comprise this workflow. The seismic alignment, the wavelet extraction, the *a priori* model and the inversion itself. After the seismic inversion the results are ready to be interpreted (anisotropy analysis). In Figure 3.4 is represented a general workflow scheme for this module.

3.1 Residual Normal Moveout (NMO) correction

Very briefly, as defined in Schlumberger Oilfield Glossary, the NMO is the effect of the separation between receiver and source on the arrival time of a reflection that does not dip. The NMO correction corresponds to the flattening of the primary reflections, removing the NMO effect from the traveltime [19].

The first major step to produce a quality inversion is to make sure the data quality is good. This implies analyzing the seismic data cubes, the available horizons and logs from the wells to make sure all information is coherent. In the azimuthal module several azimuthal fullstack data cubes will be used, which represent images from the same events only changing the azimuth at which they were acquired. During processing, the gathers have already been through the NMO correction to be flattened before stack, however, at fine scale, it is common to observe that some events are slightly shifted from stack to stack. In this case a new NMO correction (called residual NMO) must be applied to correct seismic misalignment between the different azimuthal seismic data.

3.2 Wavelet extraction

The extraction and optimization of the wavelet is an essential process in any seismic inversion work. This procedure can be summarized in three different stages:

- A first step, where an auto-correlation process is used to extract a zero-phase wavelet and a cross-correlation process is used to estimate and remove the random noise (Figure 3.1).
- A second step where, in addition to the seismic, well data as well as the preliminary zero-phase wavelets will be used to analyze the correlations between synthetic traces at wells and seismic traces. This procedure creates a wavelet for each azimuthal stack;
- A third step in which a common location for all stacks is given for each well, based on the absolute time-shift, correlation coefficient and standard deviation attributes.

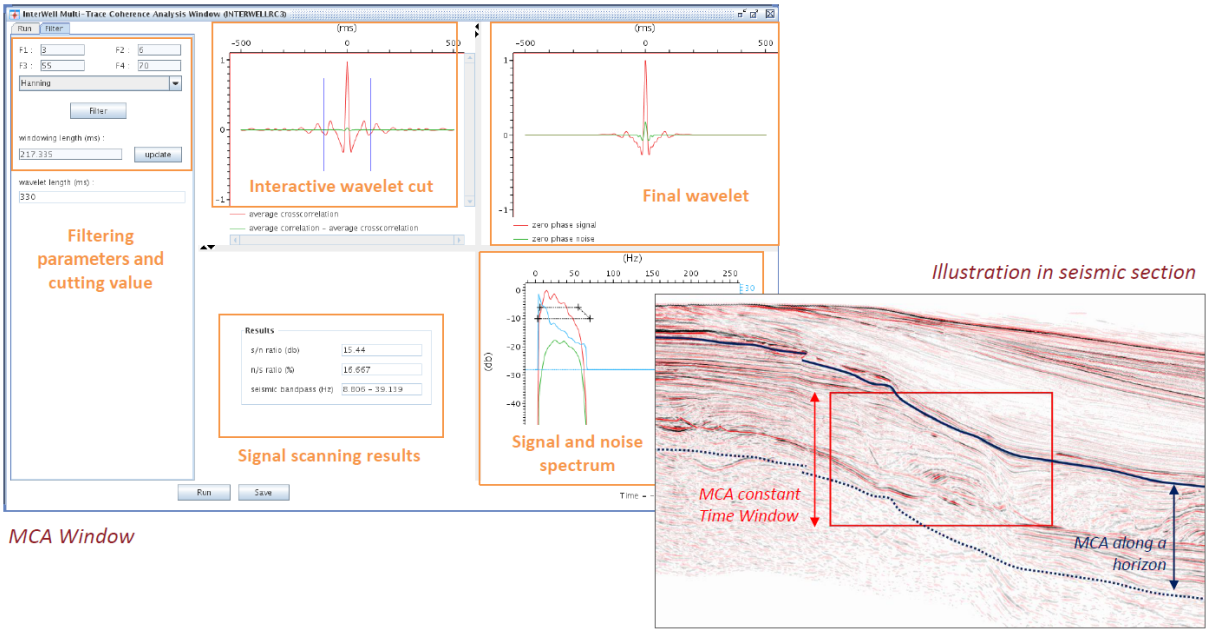

Figure 3.1: Example of a Multi-trace Coherency Analysis (MCA) window in InterWell® (Beicip-Franlab), where a zero-phase wavelet is extracted.

The normal methodology for the wavelet extraction implies the use of different wavelets, unique for each azimuthal stack. However, using different wavelets in theory should induce unwanted artificial anisotropy during the inversion process. To test this hypothesis, four wavelet scenarios are proposed and explored. The first is to use the original workflow as a comparison basis, this is, using a different wavelet per stack as originally designed. The second scenario is to choose one of the wavelets extracted and use it for all stacks. All the wavelets should be very similar since they represent the same events, so an arbitrary choice should not make any difference. The third scenario is to perform an average of all the wavelets and use it for all stacks. Finally, the fourth and last scenario is to compute an average of the azimuthal seismic stacks, thus creating a fullstack, and extract a single wavelet from it. This wavelet will then be used for all stacks during the inversion. The purpose of three different scenarios using the same methodology (single wavelet for all azimuthal stacks) is merely to find if some is more adequate than the others.

3.3 *A priori* model

The MAZ inversion module is a model-based inversion, and so uses an *a priori* model to bring the low frequency component missing from the seismic by incorporating stratigraphic information and is used as a constrain during the optimization process of the inversion. To create a model, first its necessary to define the geometrical framework, this is, create a structure by setting the horizons and defining the depositional modes to define the different layers. When the stratigraphic context is set the model can be created by interpolating the log data values between well locations and along correlation lines.

3.4 MAZ seismic inversion (Sequential inversion and Joint inversion)

Having the seismic aligned, the correspondent wavelet and the a priori model the conditions are set to proceed to the deterministic model-based inversion designed for the MAZ seismic data. Two inversion sub-types are available in this module, one that performs the inversion on each stack individually, resulting in different outputs per stack (i.e. sequential inversion), and another that combines all stacks delivering only one output for the entire inversion (i.e. joint inversion).

Sequential inversions are multi-channel model-based inversions that optimize the impedance distribution of each stack individually, resulting in different impedance volumes (equal to the number of stacks) that posteriorly to the inversion can be analyzed regarding the intensity and orientation of the anisotropy through ellipse fitting because each stack remains unique and so anisotropically different from the others. This way, sequential inversions are considered to retain not only the isotropic contribution but also the anisotropic contribution as each output corresponds to a unique stack. Joint inversions are also multi-channel model-based inversions but combine all azimuthal stacks in the inversion, and so, the single output only retain the isotropic contribution of the available seismic volumes, the similar part of all stacks. For this reason, the output of the joint inversion is considered to reflect only the isotropic contribution of the azimuthal seismic data. By subtracting the sequential and joint inversions results a residual impedance value which corresponds to the anisotropic contribution of each stack (Figure 3.2).

The sequential inversion, as said before, provides the anisotropic contribution and therefore is the origin of the intensity and orientation of the anisotropy in the results. Together with the joint inversion, the sequential inversion allows to compute residual impedance values specific to each sector. However, using only sequential inversions is possible to obtain different tools associated to seismic anisotropy, for instance, the anisotropy ratio, anisotropy error, tilt, and eccentricity (Figure 3.3). InterWell® (Beicip-Franlab) uses ellipse fitting method to evaluate the anisotropy. The intensity of the anisotropy is given by the ratio of the ellipse axe lengths and by the eccentricity (Equation 3.1) and the orientation of the HTI anisotropy is given by the ellipse longest axe, the isotropy axis, parallel to the fractures (Figure 2.3).

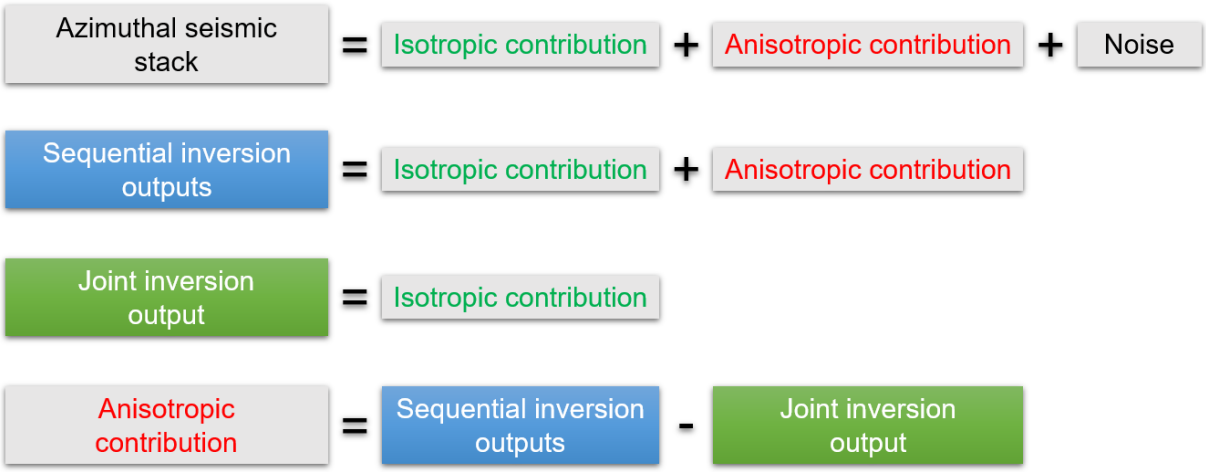

Figure 3.2: Azimuthal analysis to quantify HTI anisotropy. In an HTI media, seismic information in each azimuthal sector can be written as presented in top equation. The sequential inversion of each sector (equivalent to acoustic inversion) allows to clean the seismic data. The joint inversion of all sectors gives access to isotropic contribution. The anisotropic contribution specific to each stack is obtained by subtracting sequential and joint inversions results.

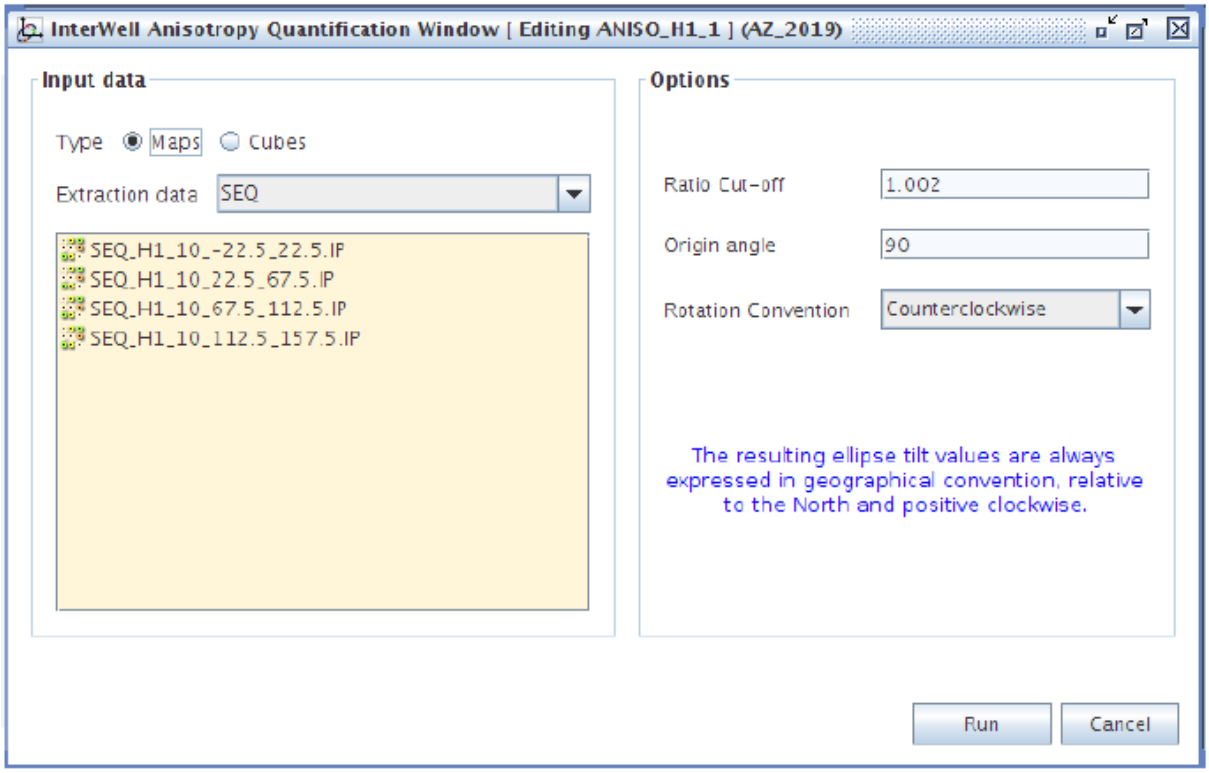

Figure 3.3: Anisotropy quantification module window in InterWell® (Beicip-Franlab).

$$e^2 = 1 - \frac{b^2}{a^2}, \tag{3.1}$$

where *e* stands for eccentricity, *b* for the ellipse short axis and *a* for the ellipse longest axis.

One challenge, however, is the choice of parameters to use when performing the sequential and joint inversions. The parameters are the impedance standard deviation (ISD) and the seismic noise/signal ratio. Both the parameters regulate the weight of seismic and the *a priori* model to be used during the inversion.

Because the inversions (sequential and joint) are different and done separately the parameters used in one might not serve to the other. This occurs because the sequential inversion processes one stack at a time while the joint inversion processes them all together. It is therefore needed to find a link between them that provides good compatibility since both outputs are combined afterwards to make anisotropy related estimations. The parameter optimization will be one of the most important and challenging tasks to complete in the entire workflow.

Both inversions (sequential and joint) use the exact same inputs (wavelet, *a priori* model and seismic sectors) and follow the same lines except for the ISD parameter which will be progressively modified to obtain optimal values. The inversions ran with a high iteration count (60 iterations) to allow the stabilization of the cost function.

Finally, the results found in the inversions will be used to perform the fracture characterization of the survey area, adding the knowledge uniquely provided by the azimuthal workflow and assessing its usefulness. In Figure 3.4 is presented a schematic describing the MAZ methodology.

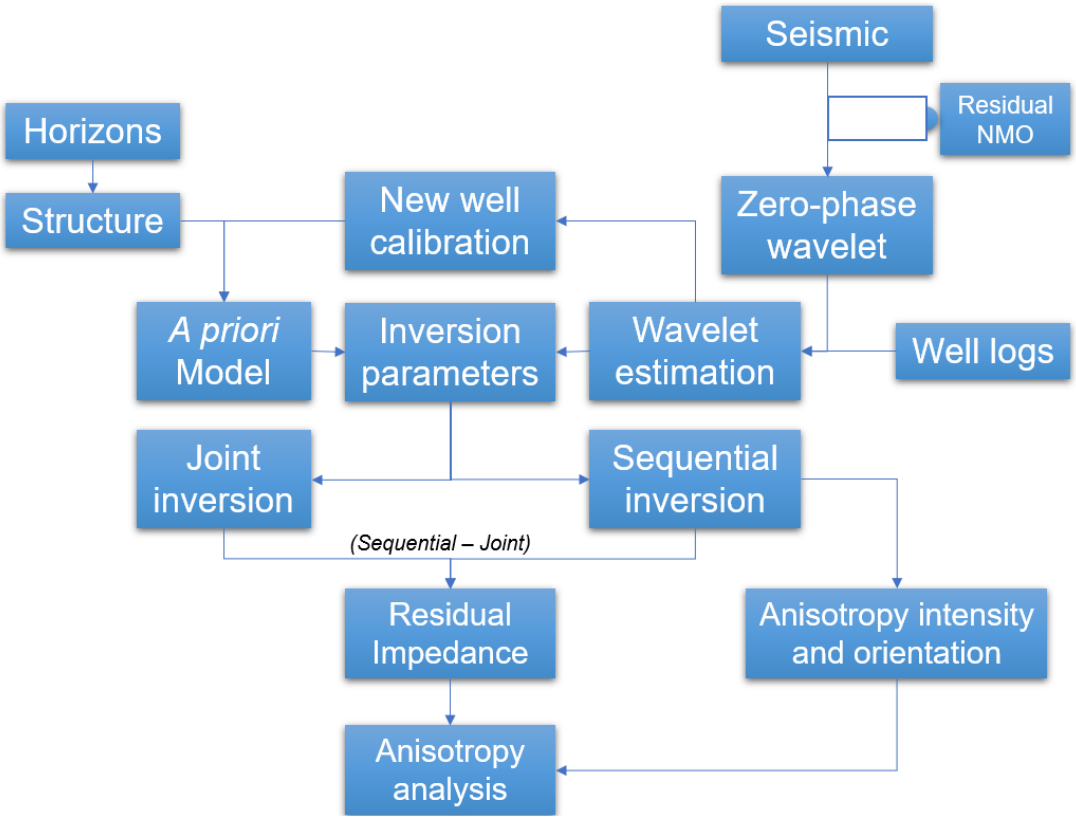

Figure 3.4: General workflow diagram for MAZ inversion methodology.

3.5 Parameter Optimization

To use the sequential and joint inversions all together in the anisotropy analysis, the output of both processes must be similar in terms of details and signal to noise ratio. To search for a relationship between the parameters of both inversions a study on how to link them was developed. First, both sequential and joint inversions, as mentioned before, are model-based inversions, and as such they work in the same way of the standard inversion in InterWell® (Beicip-Franlab). In a model-based inversion the *a priori* model is convolved with the wavelet to obtain a response which is compared with the seismic and constantly updated until the seismic response fits the seismic data upon some determined criteria where the errors are minimized (Section 2.2). The inversion parameters will define the balance between seismic and model. To link both inversions is necessary to have this seismic/model balance similar between them even if to reach the equilibrium different parameters must be used for each inversion. The parameters used to assess this relationship are the ISD and the Seismic noise/signal (Section 3.4).

The methodology used to link both inversions was simply to keep the Seismic noise/signal value to default and experiment with ISD to find which set of values are needed. Because both parameters represent the seismic/model balance, working them simultaneously would be much harder and for that reason one is kept fix in the default value while the other is being experimented. The starting point was to use the same set of parameters on both inversions and then progressively increase one or the other until the difference between the impedance on both inversions is minimum. Another important parameter to keep track is the Cost Function, this indicates the convergence of the inversion by pointing the percentage of seismic and therefore model that was used.

Chapter 4

Application and results

The fourth chapter is dedicated to the presentation of the results. The parameter optimization process will be explained and using these results the chapter will conclude with a analysis regarding the origin of the anisotropy.

A geological description of the survey area is introduced in the beginning of the chapter to add a background upon which the results are interpreted.

4.1 Geological description

This study is conducted using a dataset from Kuwait, an area studied in the past by Beicip-Franlab and is concerned about the evaporitic Gotnia and Hith formations from the Late Kimmeridgian to Tithonian.

The Gotnia formation is characterized by regionally widespread deposition of cyclic evaporites. These consist of altered halite and anhydrite-limestone units that are spatially correlated throughout the area. In the most subsiding area five levels of salt and four levels of anhydrite-limestone have been observed. The lowest salt units thin over the crest of Jurassic structures, whereas thinning of the overlying units is largely related to structural drape. The Gotnia formation is overlain by the interbedded anhydrites, argillaceous limestones and minor shales of the Hith formation, a unit which marks further infill to the basin. The salt basin is subdivided into discrete depocenters with slightly different subsidence histories that affect the thickness of the Gotnia formation and its individual units. Both the Gotnia and Hith formations are considered as good caprocks for the underlying reservoirs [20][21][22].

High pore pressures are commonly found in Kuwait, in Cretaceous and late Jurassic sections. In Najmah/Sargelu (reservoir formations), the pore pressure can reach 18 ppg and even higher pressures in the overlaying Gotnia formation, where pressure values may be as high as the fracture gradient. Drilling the Gotnia formation in Kuwait is therefore known to be a challenge. The sharp contrast in lithology between salt and stiff anhydrite associated to the high pressure and temperature environment (especially in the deeper part of the basin) make drilling operations quite hazardous and pose significant threats to drilling safety [22].

As mentioned in Section 2.3, traditional forms of seismic acquisition, such as NAZ, are not suitable to properly map the subsurface in cases of high geological complexity. In Kuwait the presence of cycling evaporites from the Gotnia formation add a layer of complexity above reservoir level. Furthermore, the proper identification of the fracture system is of utter most importance since very high pore pressure values are characteristic of the overlaying formations to the reservoir. MAZ seismic acquisition offers a good response to the geological challenges of the area by providing quality subsurface illumination and fracture characterization.

4.2 Data description

The used dataset originates from Kuwait and has inlines ranging from 27799 to 29499 and xlines ranging from 103699 to 105199. The time interval is from 1000ms to 3000ms and the sample rate is 4ms. The survey also has available twenty wells used for the wavelet estimation and *a priori* model.

4.3 Wavelet application

Different approaches regarding the way the wavelet is applied for azimuthal inversion in InterWell® (Beicip-Franlab) were explored. Three scenarios were proposed where a single wavelet was considered for all azimuthal stacks instead of different wavelets per stack, to minimize any artificial anisotropy. However, the main objective was to evaluate the single versus multiple wavelet scenario, and not the differences between the new scenarios themselves.

Further testing demonstrated that between all the single wavelet scenarios the differences were minimal, and so, the option used to carry on the inversion was the second scenario where a wavelet from one of the azimuthal stacks was used for all the others as well. The second scenario was chosen not only to reduce any artificial anisotropy but also because was the easiest to implement in the single wavelet scenario. Figure 4.1 summarizes all the scenarios.

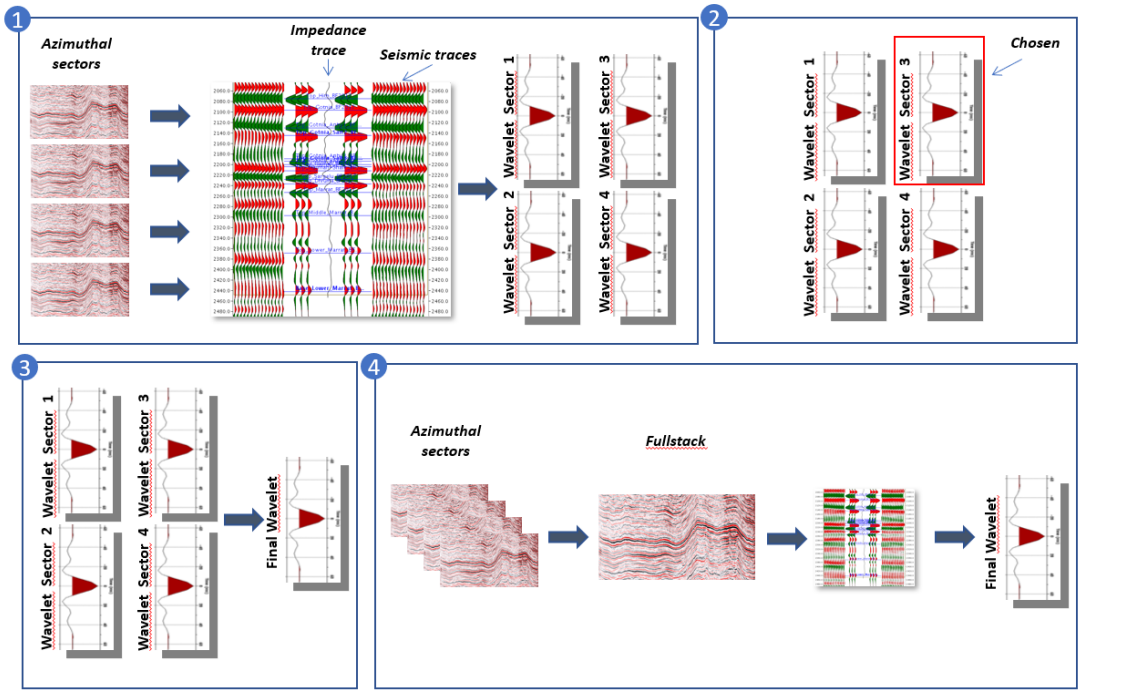

Figure 4.1: Different wavelet approaches. 1- Standard approach, one wavelet per seismic sector. 2- Only one wavelet is chosen from all available. 3- Mean of all wavelets. 4- Wavelet is extracted from a fullstack.

4.4 Multi-Azimuth seismic inversion workflow

In InterWell® (Beicip-Franlab) the Multi-Azimuth module works with seismic stacks, also called sectors (four in this work), each provided by the different shooting directions (as explained in Section 2.3). There are also two inversion workflows specific to be used with the seismic data, one to estimate the maximum/ minimum impedance values per sector and another to capture the anisotropy (intensity and orientation) using ellipse fitting.

To apply these specific workflows the MAZ module provides two types of model-based inversions. One that combines all the sectors into just one inversion (joint inversion), and another that inverts each sector independently providing an output per sector (sequential inversion) which in fact is the standard acoustic model-based inversion but done sequentially for all sectors.

The first workflow is dedicated to compute the residual impedance values in order to provide information on impedance anomalies in each sector. This is accomplished by subtracting the joint inversion from each specific sequential inversion and therefore obtaining the impedance variation of each sector when comparing to the “average” joint inversion. Information on residual impedance can be used to identify anisotropic anomalies specific to a sector. The second workflow is dedicated to capture the intensity and orientation of the anisotropy by using only the sequential inversion (as illustrated in Figure 3.4 with the first workflow as *residual impedance* and the second workflow as *anisotropy intensity and orientation*).

Both the sequential and joint inversions are necessary for the anisotropy analysis and use the same wavelet methodology described in the second scenario (Section 3.2 and Section 4.3). All inversions done further in this thesis use this methodology.

4.5 Results

One challenge when performing the inversion in the multi-azimuth module is to link the sequential and joint inversions. Since they are different optimization problems, it is expectable that the parameters to be used also differ. This problem complicates the application of the first workflow, where the objective is to obtain the residual impedance values, because to achieve optimal results both inversions must be as similar as possible so that the final impedance is the actual difference between them.

4.5.1 Parameter Optimization

Several attempts were made to find a set of parameters that produce equal results on both inversions (sequential and joint). The standard value for the ISD is 800 and a range of values between 400 and 1600 were tested, with either the parameter equal in both inversions, higher value in sequential inversion or higher value for the joint inversion. The relevant results are displayed in Figure 4.2.

Looking at the residual impedance result from Figure 4.3, with a similar parametrization the outcome is not satisfactory. Too much impedance is still displayed and a clear displacement in the cost function indicates substantial differences with the inversions (25.8%), where the sequential inversion relies much more on the a priori model then the Joint inversion.

By increasing the ISD, the weight of the seismic will also increase and the difference in the cost function will be reduced. However, the results still reveal a strong impedance presence that tends to accentuate due to one inversion being more sensitive than the other when boosting this parameter.

The parametrizations 2 and 3 (Figures A.1 and A.2) confirm that by using similar parameters on both inversions is not possible to obtain the expected outcome, no matter the seismic/model weight. The next step is to differentiate the inversions parameters until a link is found. The procedure was to imagine a relationship in the ISD parameter (sequential ISD / joint ISD) between both inversions (will be called ISD ratio) to find logic in the parameters to use. The ratio started with 1 (sequential ISD = joint ISD) (Figure 4.3) followed by a decrease and increase of the ratio to search for the most suitable combination.

By increasing the weight of the joint inversion in relation to the sequential inversion is possible to notice a strong residual impedance presence which accentuates with increasing the difference between the inversions (decrease of the ratio value). This is visible in parametrization 4 (Figure 4.4), with a ratio of 0.67 and in parametrization 5, (Figure 4.5), with a ratio of 0.5 (joint ISD parameter is twice the sequential ISD parameter). These results are clearly not the objective of this exercise and so the hypothesis of using a joint inversion with higher ISD parameters is cast aside.

ISD Ratio (Sequential/Joint)	Parametrization	Inversion	ISD	Seismic N/S	Cost Function	Cost Function difference
1	1	Sequential	400	10	44,26%	25,80%
		Joint	400	10	70,06%	
0,67	4	Sequential	800	10	70,27%	17,71%
		Joint	1200	10	87,98%	
0,5	5	Sequential	400	10	44,26%	39,66%
		Joint	800	10	83,92%	
1,3	6	Sequential	1600	10	85,91%	2,07%
		Joint	1200	10	87,98%	
1,5	7	Sequential	1200	10	80,74%	3,18%
		Joint	800	10	83,92%	
2	9	Sequential	1200	10	80,74%	1,30%
		Joint	600	10	79,44%	
3	12	Sequential	1200	10	80,74%	10,68%
		Joint	400	10	70,06%	
4	13	Sequential	1600	10	85,91%	15,85%
		Joint	400	10	70,06%	

Figure 4.2: Parametrization inversion settings

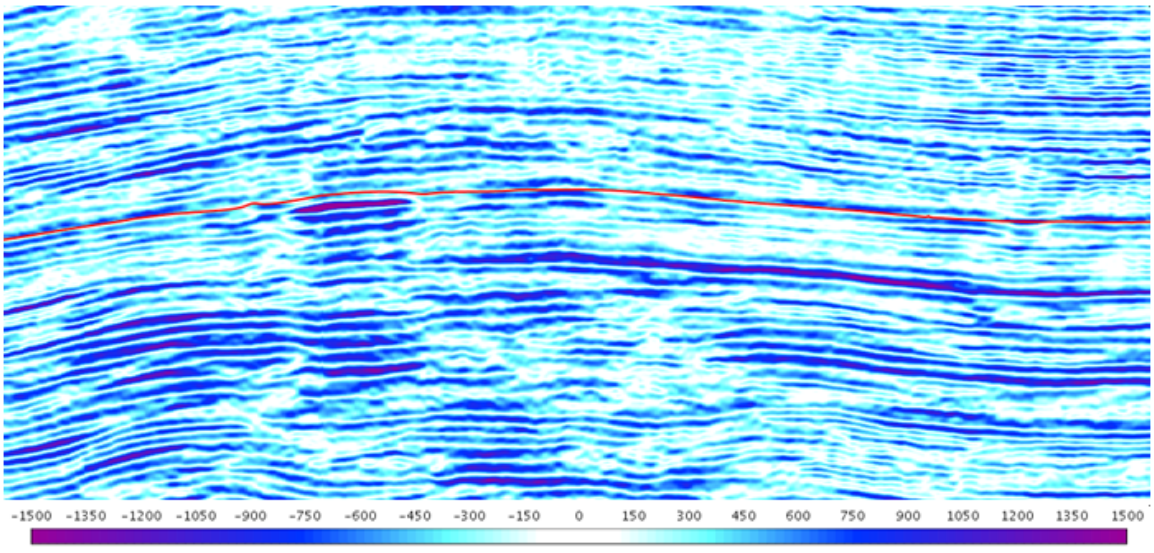

Figure 4.3: 1st parametrization residual xline cross-section of the target area (1800ms - 2800ms), performed by subtracting the results of one inversion from the other (sequential - joint).

In fact, is logical the need of the sequential inversion to use higher ISD parameters then the joint inversion. In the cases with equal parameters it was systematically observed lower values in the cost function for the sequential inversion which indicated more weight on the model, and so, less on the seismic. To accomplish similar results to the joint inversion an increase in the seismic weight is needed in the sequential inversion.

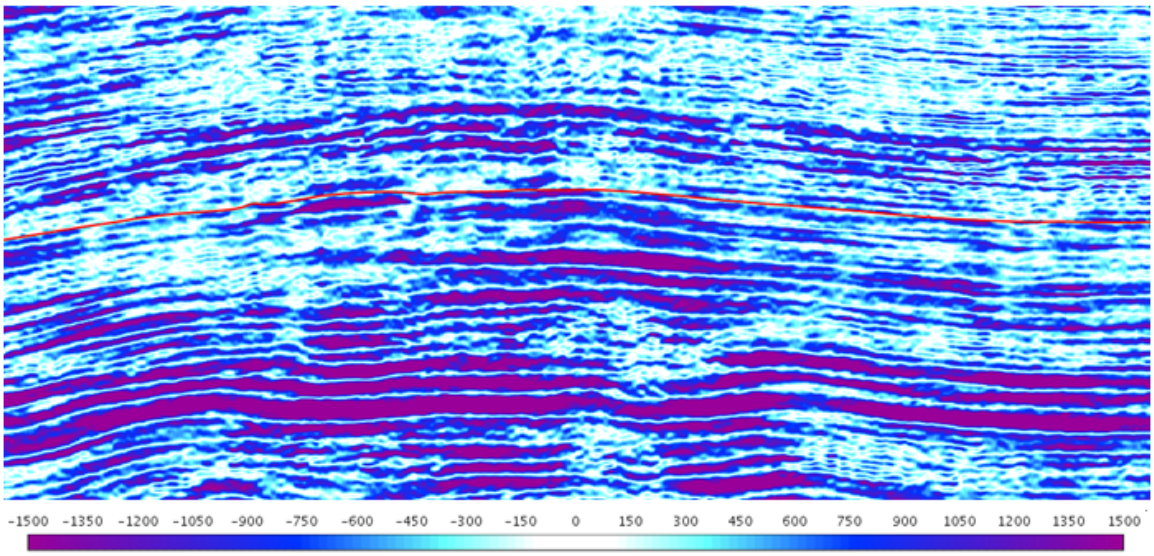

Figure 4.4: 4th parametrization residual xline cross-section of the target area (1800ms - 2800ms), performed by subtracting the results of one inversion from the other (sequential - joint).

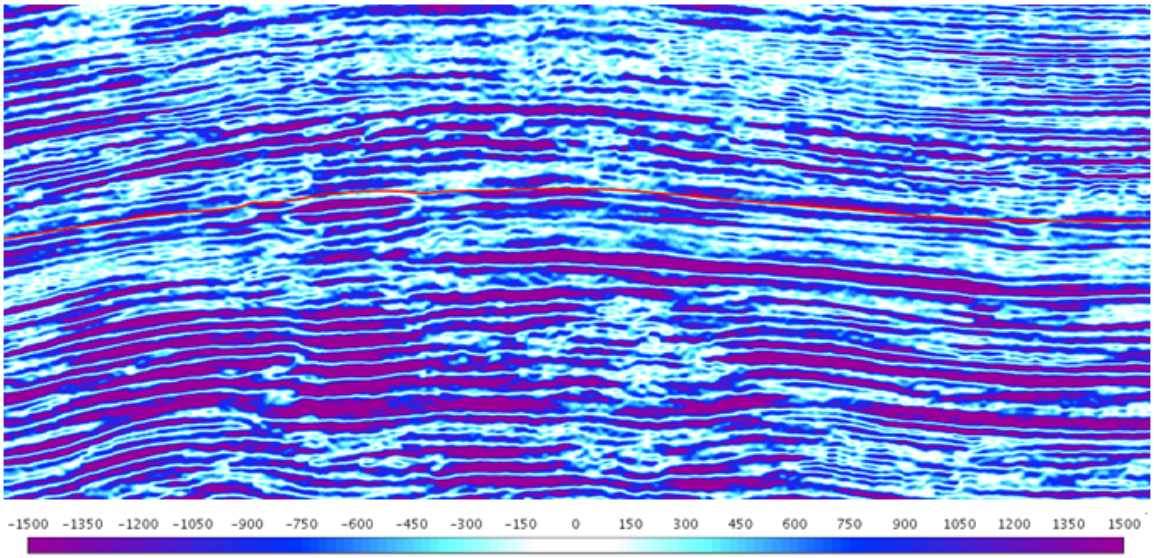

Figure 4.5: 5th parametrization residual xline cross-section of the target area (1800ms - 2800ms), performed by subtracting the results of one inversion from the other (sequential - joint).

When increasing the seismic weight on the sequential inversion and closing the gap in the cost function between both inversions the residual values immediately become promising. Parametrization 6 (Figure 4.6) with a ratio in the ISD parameter of 1.33 it is clearly an improvement comparing with the previous scenarios. Furthermore, in parametrization 7 (Figure 4.7) with a ratio of 1.5 the results are even more promising.

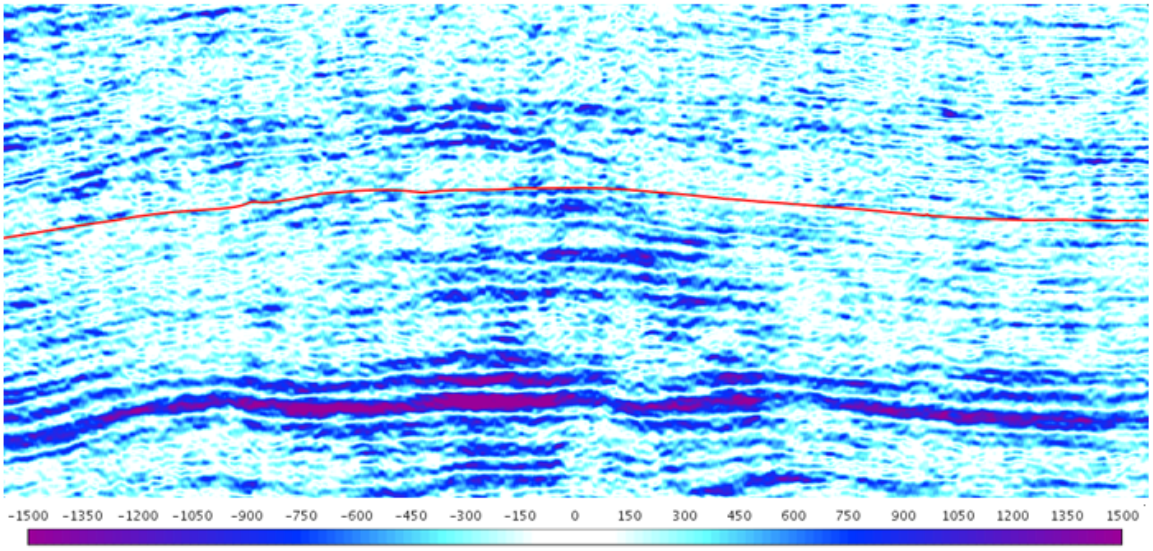

Figure 4.6: 6th parametrization residual xline cross-section of the target area (1800ms - 2800ms), performed by subtracting the results of one inversion from the other (sequential - joint).

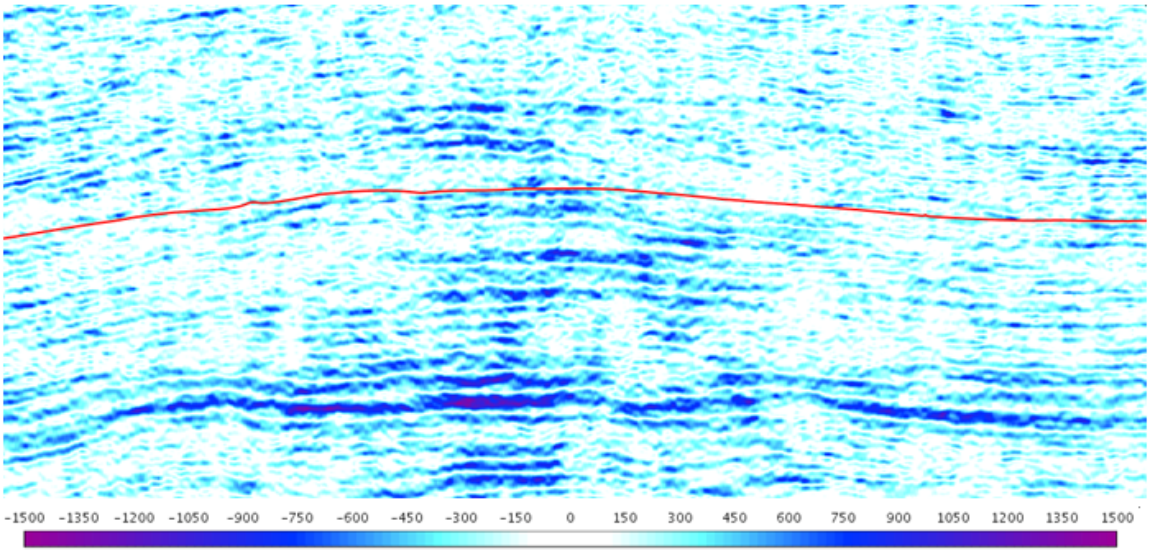

Figure 4.7: 7th parametrization residual xline cross-section of the target area (1800ms - 2800ms), performed by subtracting the results of one inversion from the other (sequential - joint).

Naturally, the logical course of action is to keep increasing the ratio. At the point where the sequential inversion ISD parameter is the double of the joint inversion ISD parameter, the cost function is identical and the residual impedance values are low as seen in parametrization 9 (Figure 4.8).

Following the satisfactory results, different weights for both inversions in the ISD parameter will be tested while keeping the sequential ISD twice the joint ISD in order to evaluate the impact of the model/seismic balance (parameterizations 8, 10 and 11, Figures A.3, A.4 and A.5). By increasing the impact of the seismic on the inversion (higher ISD values) a slight increase in residual values is noted.

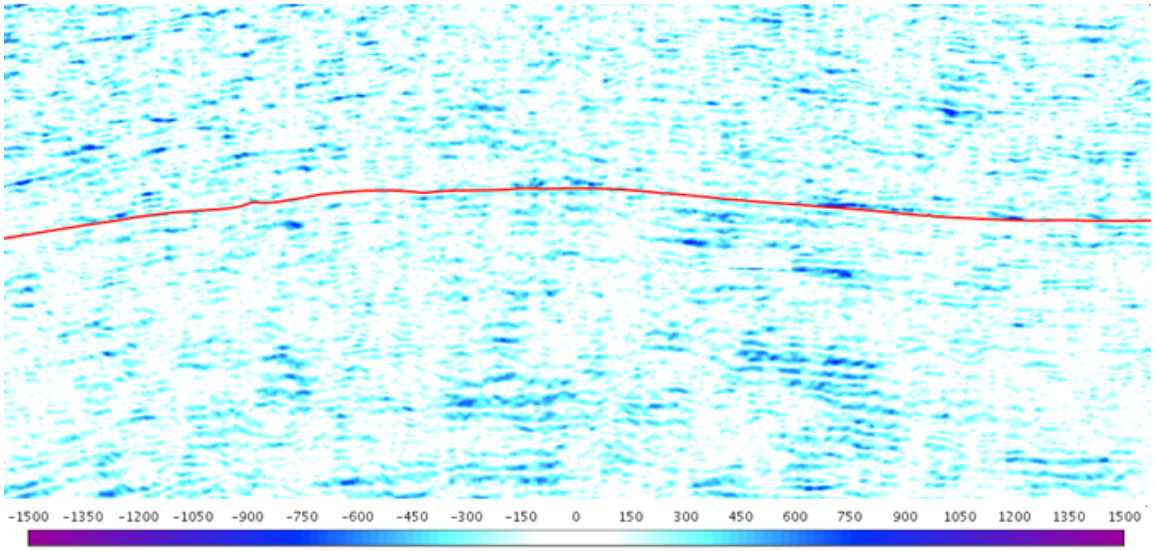

Figure 4.8: 9th parametrization residual xline cross-section of the target area (1800ms - 2800ms), performed by subtracting the results of one inversion from the other (sequential - joint).

Beyond the point where the sequential inversion is more than double of the joint inversion in the ISD parameter it is perceptible a progressive increase in residual values as displayed in parametrizations 12 and 13 (Figures 4.9 and 4.10). These results conclude that the optimal parameters where the sequential and joint inversions are most alike is when the sequential ISD is twice the joint ISD.

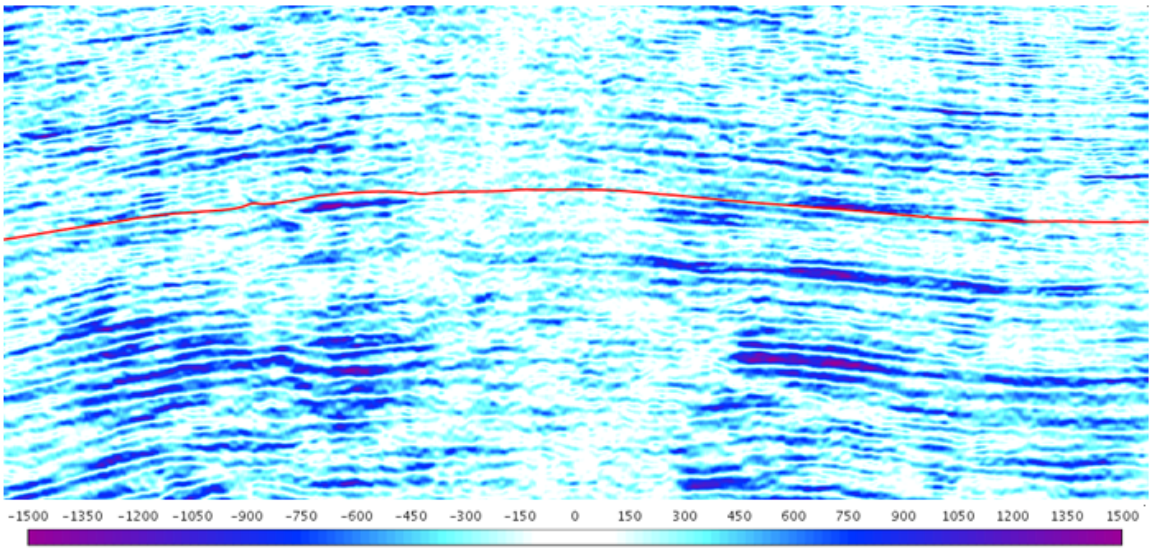

Figure 4.9: 12th parametrization residual xline cross-section of the target area (1800ms - 2800ms), performed by subtracting the results of one inversion from the other (sequential - joint).

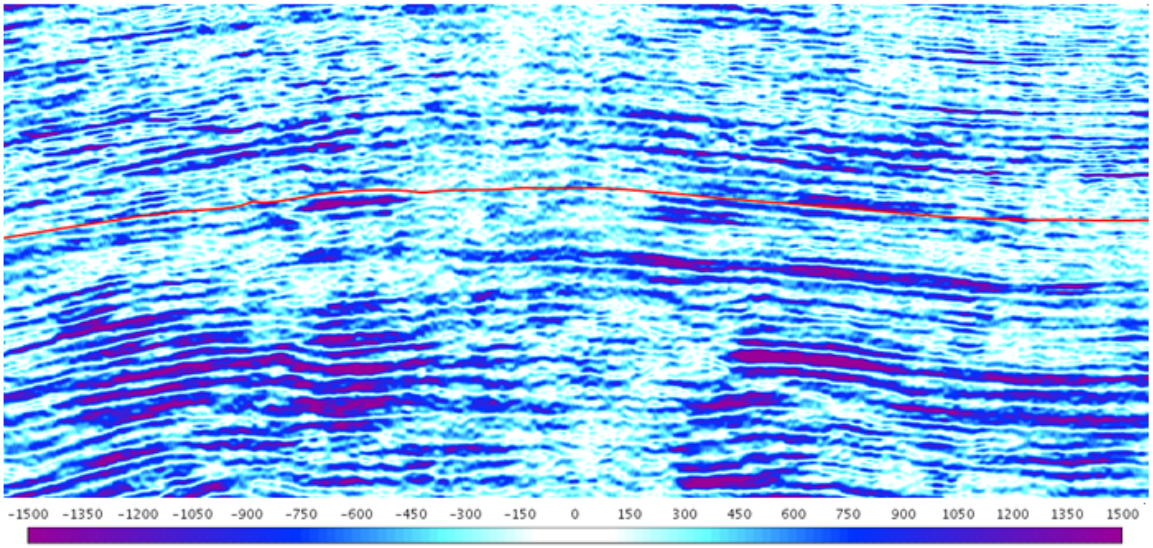

Figure 4.10: 13th parametrization residual xline cross-section of the target area (1800ms - 2800ms), performed by subtracting the results of one inversion from the other (sequential - joint).

Figure 4.11 displays the trend of the variation of the cost function with the ISD parameter ratio. The best results happen when the sequential ISD parameter is twice the joint ISD parameter (ISD parameter ratio around 2). Based on all tested parametrizations, when the sequential ISD parameter is the double of the joint ISD parameter the difference in cost function is consistently around 1% and as showed in Figure 4.8 the residual impedance values are lower when comparing to the other parametrizations which indicate the result of both inversions are closer. Because of this, the sequential ISD parameter being the double of the joint ISD parameter is the relationship that should be used.

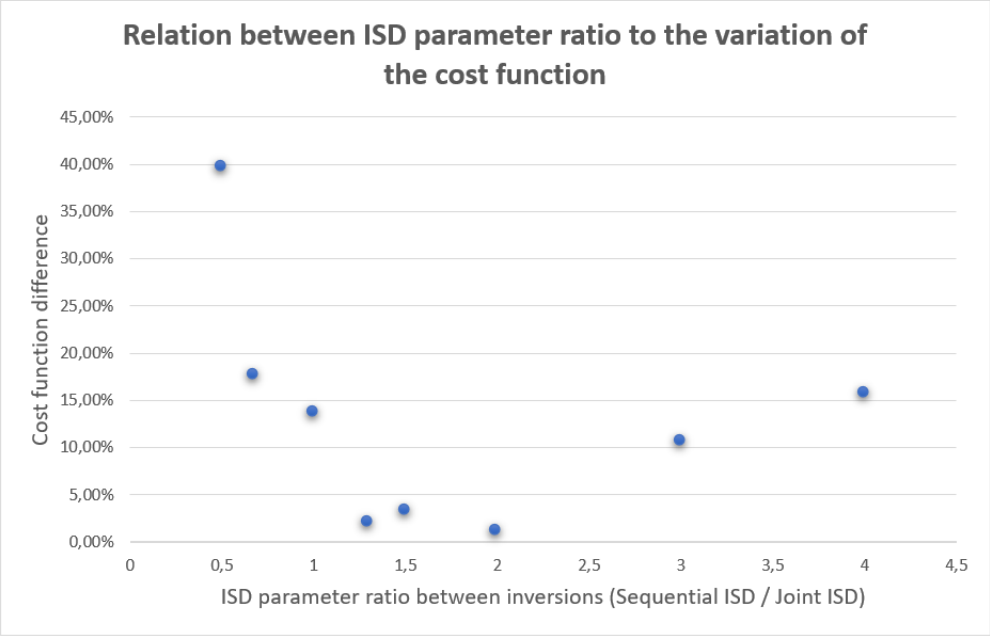

Figure 4.11: Relation between ISD parameter ratio (sequential ISD / joint ISD) to the variation of the cost function.

4.5.2 Anisotropy Quantification

There are two workflows available in InterWell® (Beicip-Franlab) software. The first one, is focused on the residual impedance values while the second provides several tools to quantify the anisotropy itself. Now, using all the resources provided from both workflows and combining them with all information available, is possible to conceive a hypothesis regarding what is in the origin of certain anisotropic anomalous areas.

In the second workflow only sequential inversions are required, through them the software provides the user with tools to identify anisotropy present in the seismic data. These tools will add a degree of confidence primarily in the identification of fractures.

At an early exploration stage, which is what is covered in this project, the focus was to roughly identify the different facies of the survey area using acoustic impedance. Since the geology is known, is valid to presume that variations in impedance over large areas correspond to variations in lithology.

Figure 4.13 displays the area of interest, at the Hith formation level, which contains major faults clearly visible using the similarity attribute tool of the software designed specifically for the detection of these primary fault networks. The anisotropy ratio (Figure 4.13), obtained from sequential inversions through ellipse fitting, and impedance (Figure 4.12) attributes are displayed together with the similarity map to have a visual representation of the faults on top of each map, this serves as a guide to correlate mainly the faults to certain impedance anomalies.

When comparing the impedance results from the sequential inversions for the four sectors along the Hith formation is visible that the impedance values tend to have spatial variations, from sector to sector. The goal is to assess if some of the anisotropy present can be explain by the impedance.

The interest in using azimuthal sectors is to understand the changes that happen from sector to sector. In this case many of the shifts in impedance correspond to the boundaries between higher and lower impedances and knowing that the Hith formation is composed mainly of anhydrites and carbonates (i.e. limestones) is expected that higher impedances tend to be anhydrites and lower impedances tend to be carbonates.

Transition areas between anhydrites and carbonates could be a factor for anisotropy and in fact, in Figure 4.12 areas A, B and C points to areas where some differences between sectors exist and when comparing the same areas in Figure 4.13 there is a match with high anisotropic ratio. The hypothesis defended here is that transition zones between lithologies (lower impedance tend to be carbonates while higher impedances tend to be anhydrites) could be a factor for anisotropy. Areas A, B and C are in white, and so transition areas where a mix in the lithology could explain the differences in impedance observed between the azimuthal sectors and the presence of anisotropy.

If some anisotropy could potentially be explained by the lithology in other cases this does not apply, at least in the same simplistic manner. The impedance values predicted for areas D and E do not appear to be influenced by the azimuth and overall seem consistent among all sectors. However, significant anisotropy is detected in these two areas. The anisotropy present here cannot be explained in the same way as the previous areas (A, B and C) and to assist in the explanation of its origin a different resource is needed.

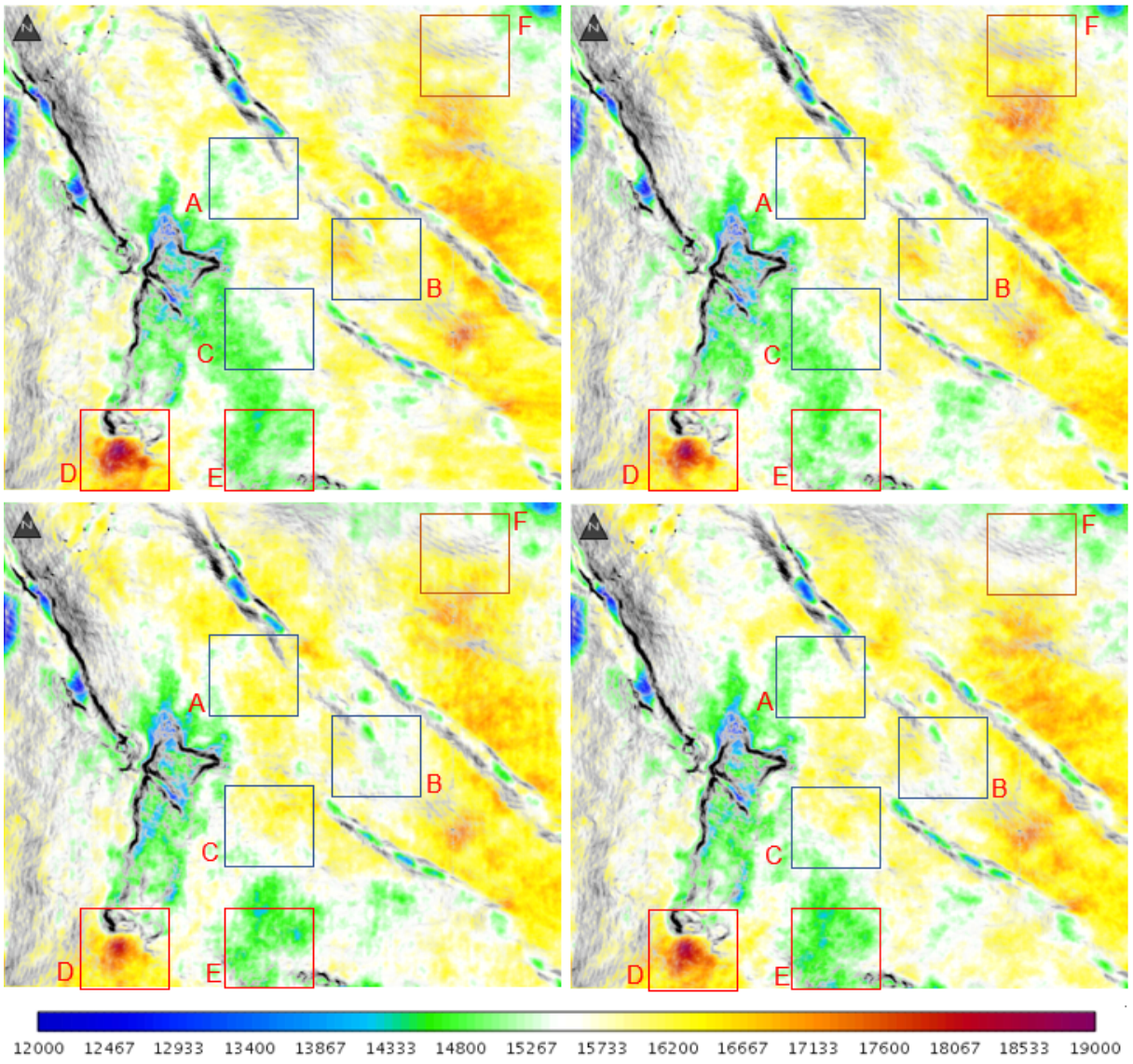

Figure 4.12: Map of the area of interest, provided by the sequential inversion, which delineates the acoustic impedance of the four different sectors, top left corresponds to the first sector, top right to the second sector, bottom left to the third sector and bottom right to the fourth sector. In all sectors are represented six subareas of interest are marked with the letters A, B, C, D, E, F.

Figure 4.14 show two maps of the residual impedances (parametrization 9, Figure 4.2), one from the first sector and other from the second sector. The key element here is the presence of high values in one area while absent in the other. This behavior indicates that when shooting from certain directions is possible to detect events (mainly fractures) in certain areas that are not detected in other shooting directions. With this knowledge is viable to associate the areas D and E to smaller fractures and so explain to some extent the high anisotropy located in certain locations.

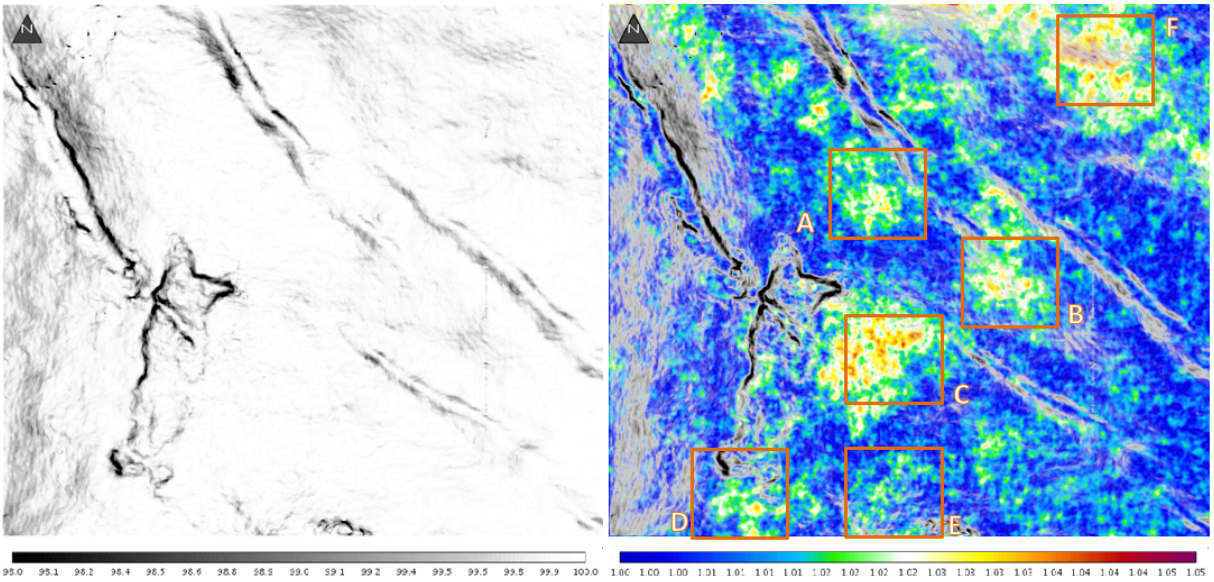

Figure 4.13: Left: Map of the area of interest which delineates the fracture system performed by the similarity tool. Right: Map of the area of interest which delineates the anisotropy ratio on top of the fracture system. Additionally, six subareas of interest are marked with the letters A, B, C, D, E, F.

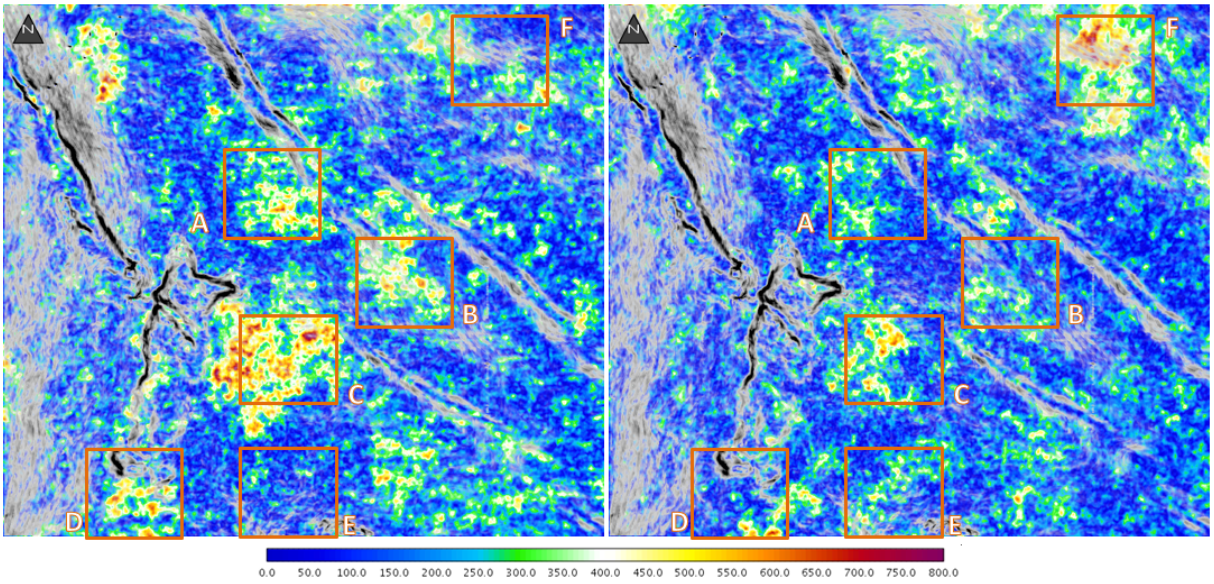

Figure 4.14: Map of interest which delineates the residual impedance values (sequential inversion - joint inversion) from the first sector (left) and second sector (right). Additionally, six subareas of interest are marked with the letters A, B, C, D, E, F.

There are other zones represented in Figure 4.14 with visible differences from one sector to the other, including in the central areas (A, B and C) where changes in lithology were previously associated as the origin of anisotropy. Is very likely the presence of smaller fractures parallel to the major ones clearly visible in the maps and in this case it justifies the higher presence of residual impedance values in the first sector as this shooting direction could favor the detection of such events. Nevertheless, the differences that occur in the central area (areas A, B and C) do not seem as abrupt as the ones in the bottom (areas D and E) since the source of the existing anisotropy is expected to be primary from the lithology.

In the top right corner of the map, in area F, there is a high anisotropy area that fits both the lithology and the partially detected fractures approach. This serves to exemplify that anisotropy could result from a variety of factors and to limit its explanation to one possible solution could be incorrect.

The assumptions made here are somewhat shallow and there should be further testing, including using well information, and other methodologies and resources to better identify and characterize the facies and fractures in the targeted area. However, by using only simple resources logical explanations regarding the origin of the existing anisotropy were given, and so, the MAZ module proves to be a valuable resource regarding fracture identification and anisotropy quantification.

4.6 Secondary results

This section is dedicated to present results that are not the main focus of the thesis. Here an alternative to the joint inversion will be proposed and the impact that using one wavelet has, or not, when comparing to the standard multi wavelet scenario will be evaluated.

4.6.1 Using the fullstack as an alternative for the joint inversion

During the process of finding the best set of parameters to obtain proper residual values an alternative was formulated to simplify the process and to reduce the higher computational requirements to perform the joint inversion. This inversion, as said before, is a combination of all sectors during the inversion itself, and therefore, requires the loading of all sectors which occupy considerable amount of memory. This alternative is particularly useful if the memory available is more limited.

The concept is very simple, instead of combining the sectors during the inversion, they will be combined before the inversion, this is, a fullstack will be created and then inverted using the standard deterministic inversion. In this way, instead of using all the seismic data from the different sectors, only one seismic dataset (fullstack) is necessary.

To test this hypothesis and confirm if this method can indeed be used, first it must be compared to the results from the joint inversion and confirmed the similarity. To proceed with the comparison the fullstack inversion and joint inversion parameters used were equal to the sequential inversion of parametrization 9 (Figure 4.2). When calculating the differences between the inversions it is obvious that they are small as observed in Figure 4.16. Besides the computationally less demanding inversion operation, this alternative to replace the joint inversion uses the same set of parameters as the sequential inversion, and so, does not require the discrepancy previously seen where the ISD parameter of the joint inversion needed to be half of the sequential inversion.

Figure 4.17 represents the differences in percentage between both inversions by considering the values of the joint inversion as 100% and measuring how much the residual varies from this value (Equation 4.1).

$$\frac{100 * (Fullstack - Joint)}{Joint}, \tag{4.1}$$

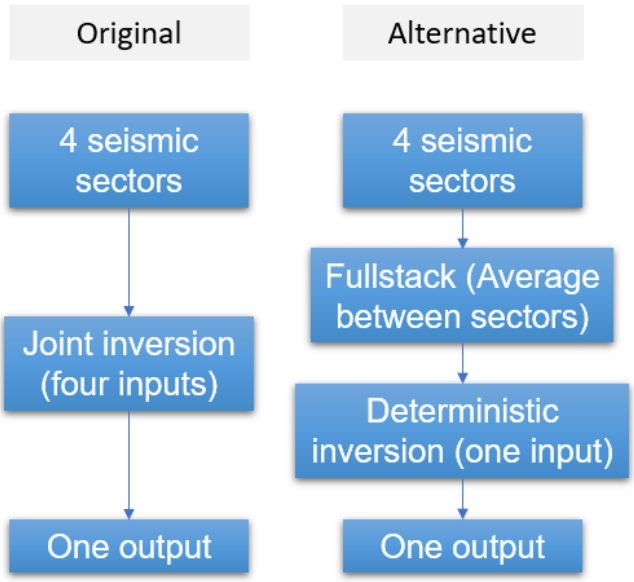

Figure 4.15: Diagram for the original Joint inversion methodology (left) and the alternative methodology using a fullstack and deterministic inversion as a replacement for the Joint inversion (right).

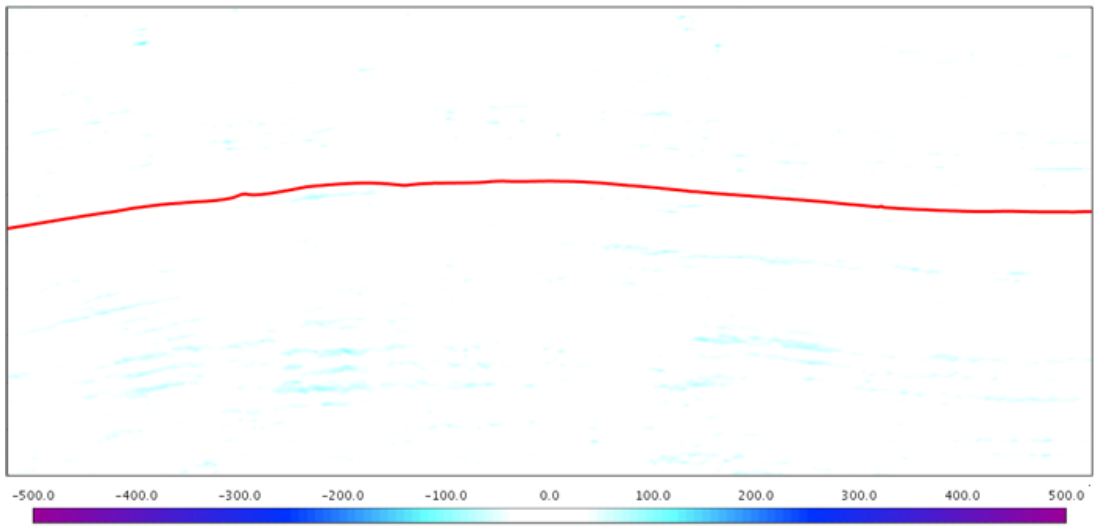

Figure 4.16: Residual xline cross-section of the target area (1800ms - 2800ms), performed by subtracting the results of one inversion from the other (fullstack - joint).

The low impedance values resulting from the difference between the fullstack inversion and the joint inversion (Figures 4.16 and 4.17) mean that in practice both are alike. Furthermore, by analyzing the statistic values of the same section is evident the irrelevance of the difference with the average difference being 0.0279% and the top differences being under 1.2% as showed in Figure 4.18.

Overall, the use of the fullstack alternative can be useful in certain situations where the user is more limited in terms of computational resources. This alternative is interesting and with further testing can have some value if properly added to the software to replace the joint inversion, however, is not a priority as it is only a workaround to obtain the same result.

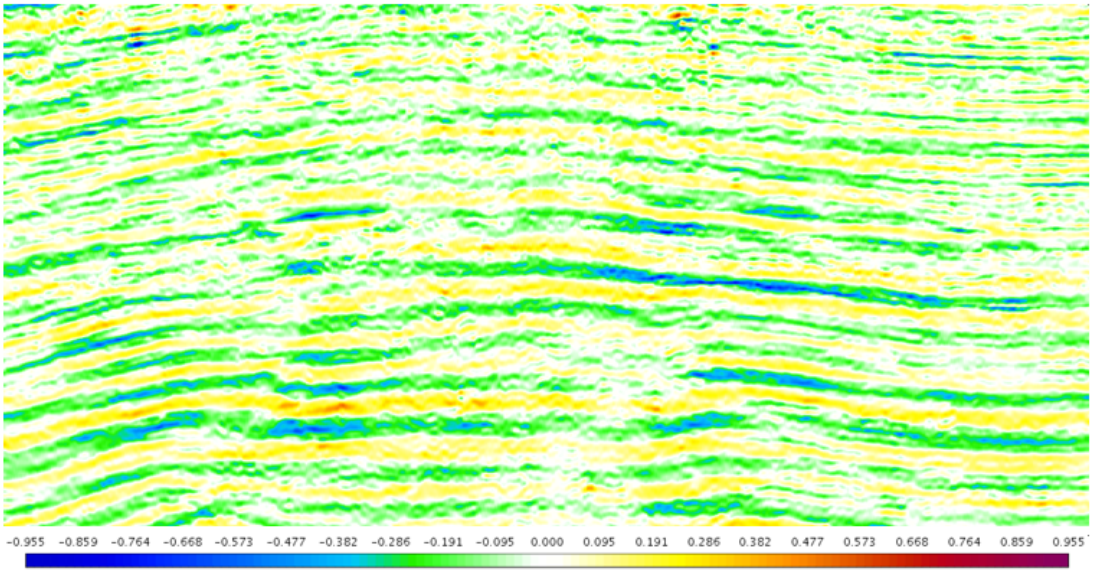

Figure 4.17: Difference in percentage between the fullstack inversion and the joint inversion on target area (1800ms - 2800ms) performed by using the operation in equation 4.1.

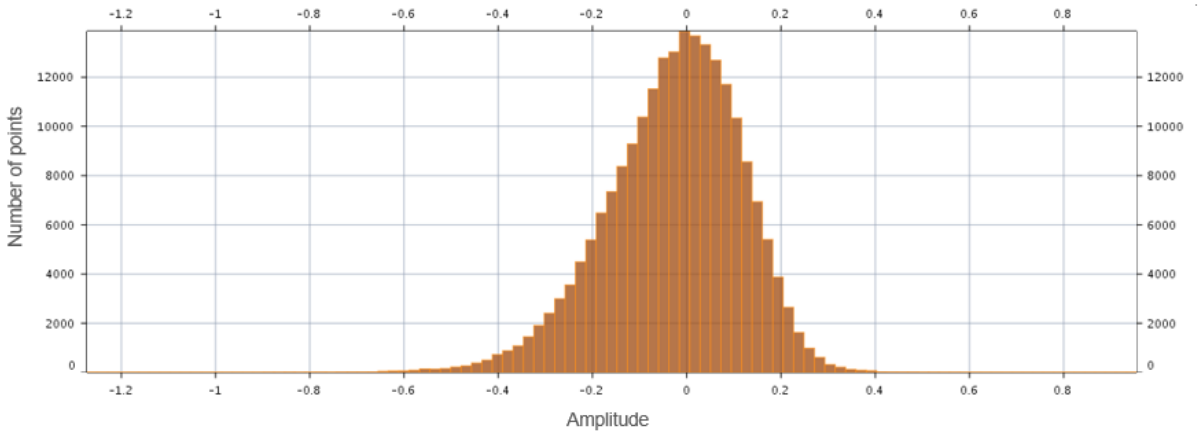

Figure 4.18: Distribution of the difference in percentage of the target area represented in Figure 4.17.

4.6.2 Wavelet influence (single wavelet vs multiple wavelets)

The wavelet approach was different from what is by default used in MAZ inversion module of InterWell® (Beicip-Franlab) as explained in Sections 3.2 and 4.3. The intention was to reduce artificial anisotropy caused by using different wavelets to represent the same seismic. In this dataset there are minor changes when using four different wavelets but overall, the results are consistent no matter the used wavelet methodology.

In Figure 4.20 are represented the residual impedance values for the second sector with a single wavelet used from scenario 2, and multiple wavelets as originally intended (Sections 3.2 and 4.3). The parameters used are equal for all scenarios based on the best acquired parametrization (9th Parametrization - Figure 4.2). For all the remaining three sectors the behavior is the same, small changes with multiple wavelets, but the overall result is the same and between single wavelet scenarios the differences are even smaller.

Figure 4.19 illustrates the anisotropy ratio using one wavelet (scenario 2) and multiple wavelets (Sections 3.2 and 4.3). The joint inversions used to obtain both anisotropy ratios had the same parameters (9th Parametrization - Figure 4.2). Just like the residual impedances the changes in the anisotropy ratios are minimal and are not significant in this dataset.

In Figure 4.21 is displayed the wavelet used to perform all single wavelet scenarios.

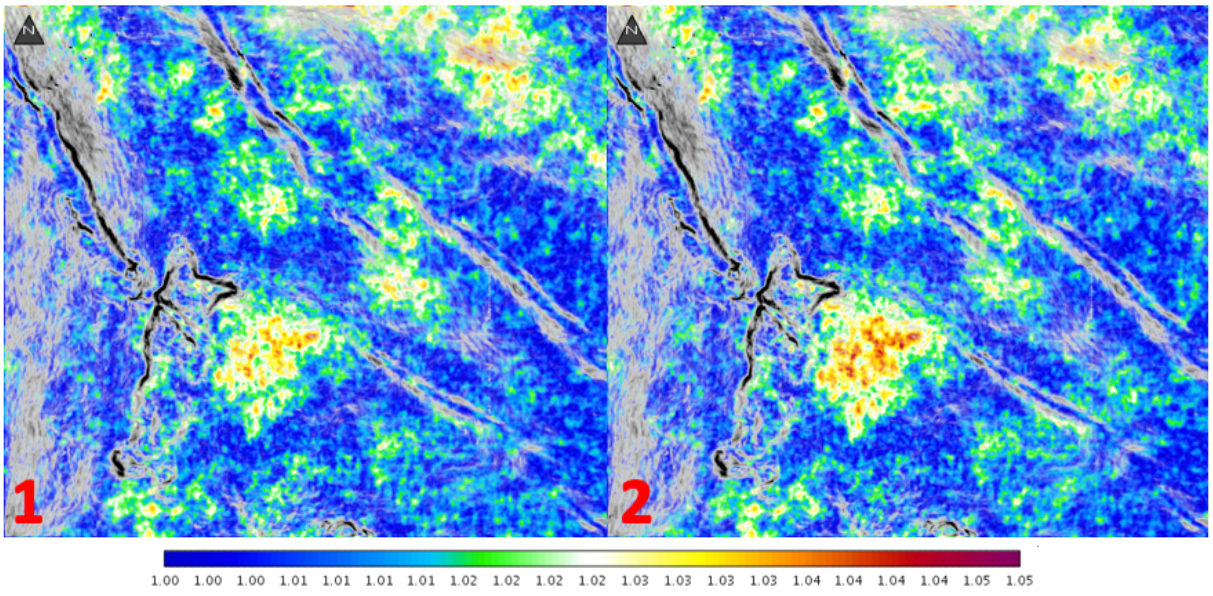

Figure 4.19: Wavelet methodology impact on anisotropy ratio. On left is displayed the single wavelet scenario while on the right the multi-wavelet scenario (Sections 3.2 and 4.3).

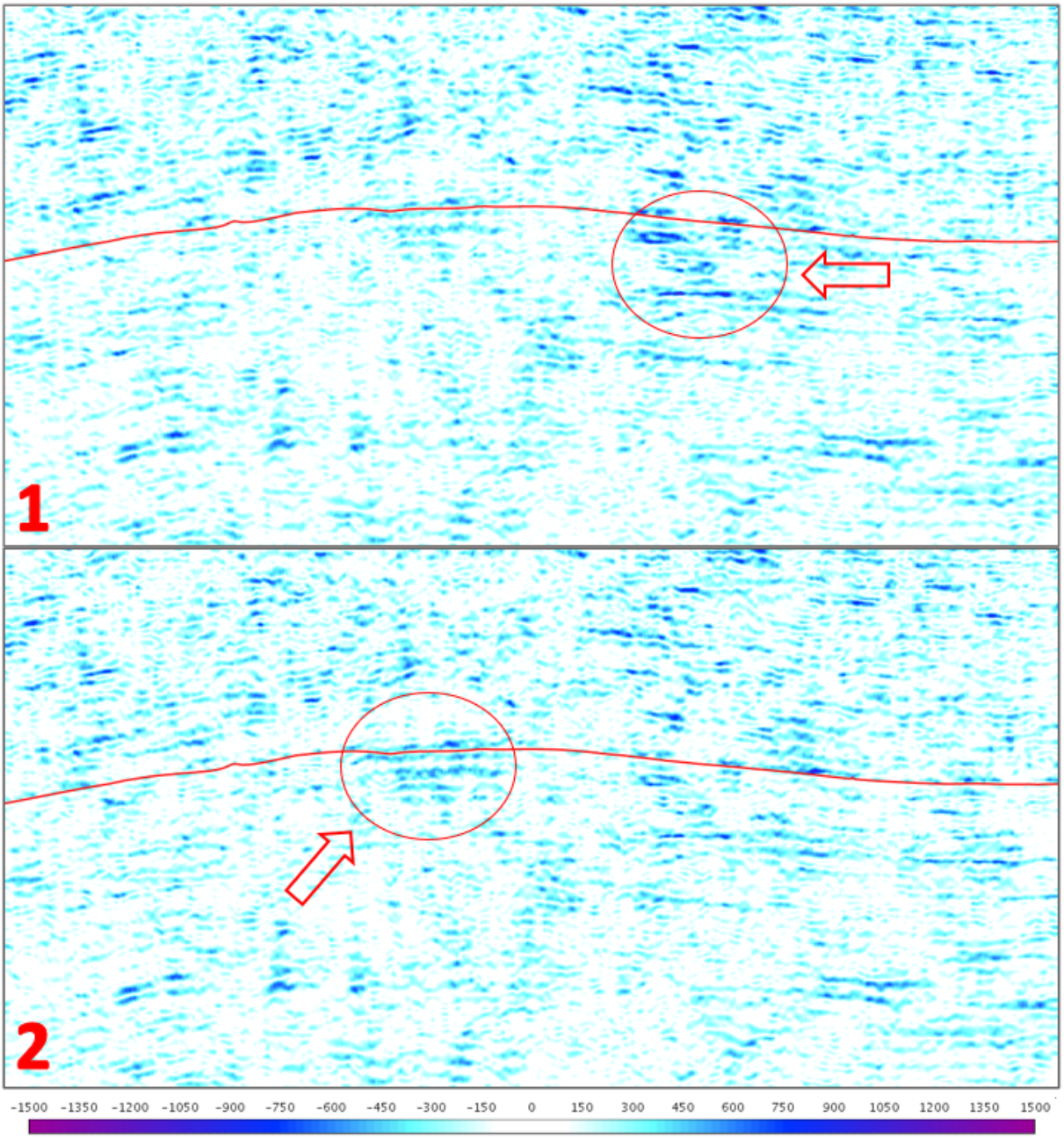

Figure 4.20: Wavelet methodology impact on residual impedance (sequential – joint) for the second sector. On top is displayed the single wavelet scenario while on the bottom the multi-wavelet scenario (Sections 3.2 and 4.3).

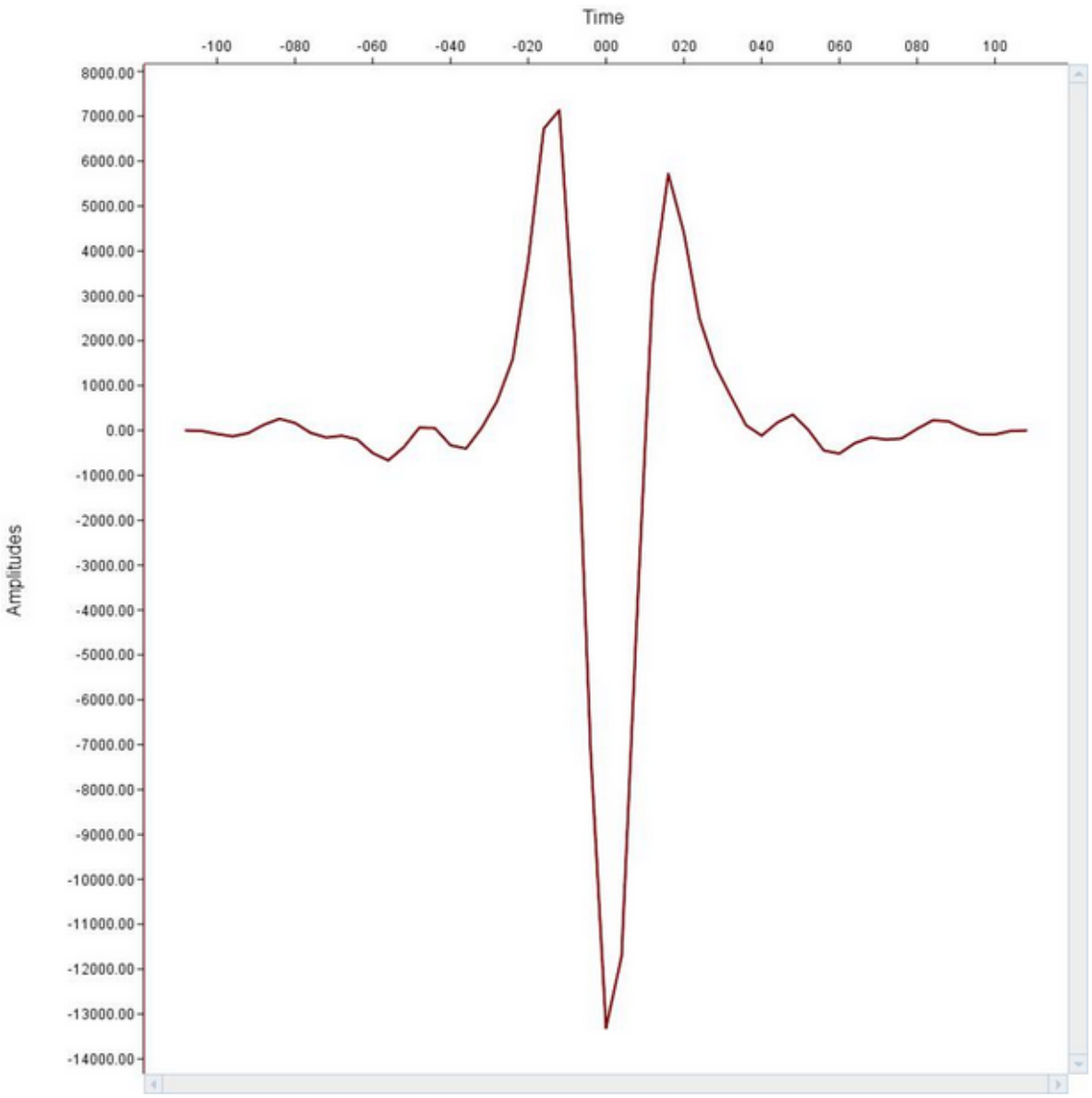

Figure 4.21: Wavelet used from second scenario (Section 4.3)

4.7 Discussion

An inversion of the seismic data was performed in InterWell® (Beicip-Franlab) with a new wavelet methodology which uses a single wavelet instead of the standard multiple wavelets in order to potentially reduce any artificial anisotropy caused by having different wavelets to represent the same event. In Subsection 4.6.2 is explained that only small variations occur between the multi wavelet methodology and all the single wavelet methodologies and therefore, based on the data alone, this modification is not considered essential.

A major challenge was to find a relationship in the parameters to use in the sequential and joint inversions. So that both inversions can be used to extract the specific impedance values of each sector the inversions had to be as similar as possible. To find the correct set of parameters to use a series of tests were performed, as described in Section 3.5, where very satisfactory results emerged when ISD parameter of the sequential inversion is about two times the ISD parameter of the joint inversion which results in cost function values very similar in both inversions (Figure 4.2) and overall low impedance values (residual impedance) when subtracting the joint inversion from the sequential inversion (Figure 4.8).

An alternative to the joint inversion was idealized to simplify parameters and to be computationally less demanding. The idea is to create a fullstack with all seismic sectors and run a standard deterministic inversion instead of the joint inversion where all sectors are combined in the inversion process (Figure 4.15). Using this method, the inversion obtained is very similar to the joint inversion, uses the same parameters as the sequential inversion and takes, in this case, a quarter of memory in the inversion process.

Following the results from the parameter optimization, an analysis regarding the origin of the anisotropy was performed. The hypothesis presented was that the source of the anisotropy could primarily come from either the lithology or a smaller system of fractures. The impedance maps from Figure 4.12 indicate three areas (A, B and C) where the lithology transits between lower impedance carbonates and higher impedance anhydrites. These three areas change considerably in each sector and correspond to high anisotropic values (Figure 4.13) and so, part of the anisotropy could come from the transition between lithologies. Also from Figure 4.12 areas D and E appear to be stable in terms of impedance, however, in Figure 4.13 correspond to a high anisotropy ratio. This excludes the lithology as the anisotropic source for these areas and by looking into the residual impedance (sequential inversion - joint inversion) in Figure 4.14 is visible that both areas are better detected in a specific sector and less in the other. This indicates a possibility of having fractures invisible to a shooting direction and visible to other, and therefore, the source of the anisotropy in these areas is assumed to be a small fracture system. In area F there is a high cluster of anisotropy (Figure 4.13) with considerable variations in impedance (Figure 4.12) and also in residual impedance between sectors (Figure 4.14) which indicate that both the lithology and fractures could explain the high anisotropic values.

Chapter 5

Conclusions

This thesis addresses the topic of seismic anisotropy and how azimuthal seismic data can be processed to support a better interpretation of the subsurface. By using multi-azimuthal seismic data is possible to map in detail complex geological structures and to determine the source of the detected anisotropy.

In this work the objective of improving the methodology for the multi-azimuth seismic inversion was achieved, even though the wavelet methodology did not had a significant impact the parameter optimization provided solid information on how to proceed with the sequential and joint inversions. Additionally, an alternative for the joint inversion was formulated to simplify the choice of parameters and to reduce the necessary computer memory for the inversion. Finally, hypothesis were proposed as the origin of the anisotropy in the target area possible only by using multi-azimuth seismic.

5.1 Future work

The theme exposed in this thesis is still very superficial with a large room for improvement. The wavelet methodology should be experimented with different datasets to conduct a more rigorous analysis if the impact in the results is significant or not. Also, a more in-depth study of the well data should be done to have a better understanding of the lithology to validate if indeed is a cause for anisotropy. Finally, the complete detailed interpretation and characterization of the fracture system should be the final objective and is still not accomplished.

Bibliography

[1] M. Asghari and M. A. Rakhshanikia. Technology transfer in oil industry, significance and challenges. *Procedia - Social and Behavioral Sciences*, 75:264 – 271, 2013. doi: https://doi.org/10.1016/j.sbspro.2013.04.030.

[2] B. D. Sala. Meeting challenges of the oil industry. *World Pumps*, 2015(4):28 – 29, 2015. ISSN 0262-1762. doi: https://doi.org/10.1016/S0262-1762(15)30063-8. URL http://www.sciencedirect.com/science/article/pii/S0262176215300638.

[3] R. Simm and M. Bacon. *Seismic Amplitude: An Interpreter's Handbook*. Cambridge University Press, 2014. ISBN 9781107011502. URL https://books.google.pt/books?id=1RYmAwAAQBAJ.

[4] A. Long. Evolutions in seismic azimuth: past, present and future. *Geohorizons*, page 4–14, july 2009.

[5] A. Tarantola. *Inverse Problem Theory and Methods for Model Parameter Estimation*. Society for Industrial and Applied Mathematics, 2005. doi: 10.1137/1.9780898717921. URL https://epubs.siam.org/doi/abs/10.1137/1.9780898717921.

[6] M. G. Averill, K. C. Miller, G. Randy Keller, V. Kreinovich, R. Araiza, and S. A. Starks. Using expert knowledge in solving the seismic inverse problem. *International Journal of Approximate Reasoning*, 45(3):564 – 587, 2007. ISSN 0888-613X. doi: https://doi.org/10.1016/j.ijar.2006.06.025. North American Fuzzy Information Processing Society Annual Conference NAFIPS '2005.

[7] B. H. Russell. *Introduction to Seismic Inversion Methods*. Society of Exploration Geophysicists, 1988. doi: 10.1190/1.9781560802303. URL https://library.seg.org/doi/abs/10.1190/1.9781560802303.

[8] M. Bosch, T. Mukerji, and E. F. Gonzalez. Seismic inversion for reservoir properties combining statistical rock physics and geostatistics: A review. *GEOPHYSICS*, 75(5):75A165–75A176, 2010. doi: 10.1190/1.3478209.

[9] O. Enwenode. *Understanding Seismic Wave Propagation*, pages 17–32. Seismic Data Analysis Techniques in Hydrocarbon Exploration, december 2014. ISBN 9780124200234. doi: 10.1016/B978-0-12-420023-4.00002-2.

[10] L. Azevedo and A. Soares. *Geostatistical Methods for Reservoir Geophysics*. Springer International Publishing. ISBN 978-3-319-53201-1. doi: 10.1007/978-3-319-53201-1.

[11] A. R. Brown. *Interpretation of Three-Dimensional Seismic Data, Seventh edition*. Society of Exploration Geophysicists and the American Association of Petroleum Geologists, 2011. ISBN 978-0-89181-374-3. doi: 10.1190/1.9781560802884. URL https://library.seg.org/doi/abs/10.1190/1.9781560802884.

[12] A. Cordsen and M. Galbraith. Narrow- versus wide-azimuth land 3d seismic surveys. *The Leading Edge*, 21(8):764–770, 2002. doi: 10.1190/1.1503181. URL https://doi.org/10.1190/1.1503181.

[13] A. Long, E. Fromyr, C. Page, W. Pramik, and R. Laurain. Multi-azimuth and wide-azimuth lessons for better seismic imaging in complex settings. *ASEG Extended Abstracts*, january 2006. doi: 10.1190/segj082006-001.8.

[14] R. E. Sheriff. *Encyclopedic Dictionary of Applied Geophysics, Fourth edition*. Society of Exploration Geophysicists, 2002. doi: 10.1190/1.9781560802969. URL https://library.seg.org/doi/abs/10.1190/1.9781560802969.

[15] E. Liu and A. Martinez. 2 - fundamentals of seismic anisotropy. In E. Liu and A. Martinez, editors, *Seismic Fracture Characterization*, pages 29 – 57. EAGE, Oxford, 2012. ISBN 978-90-73834-40-8. URL http://www.sciencedirect.com/science/article/pii/B9789073834408500073.

[16] S. Chopra and J. P. Castagna. *AVO*. Society of Exploration Geophysicists, 2014. doi: 10.1190/1.9781560803201. URL https://library.seg.org/doi/abs/10.1190/1.9781560803201.

[17] X. Fu, J. Yu, J. Yuan, and C. Han. Modelling analysis of the limitation of p-wave avaz inversion. *Journal of Applied Geophysics*, 170:103842, 2019. ISSN 0926-9851. doi: https://doi.org/10.1016/j.jappgeo.2019.103842. URL http://www.sciencedirect.com/science/article/pii/S0926985119300461.

[18] S. Henry. Catch the (seismic) wavelet. *Geophysical Corner*, pages 36–38, march 1997.

[19] D. Dondurur. *Normal Moveout Correction and Stacking*, pages 459–492. Acquisition and Processing of Marine Seismic Data, 01 2018. ISBN 9780128114902. doi: 10.1016/B978-0-12-811490-2.00010-4.

[20] M. Al-Husseini. Jurassic sequence stratigraphy of the western and southern arabian gulf. *GeoArabia*, 2:361–382, 01 1997.

[21] M. Rahaman, A. Hafez, Y. Al-Zuabi, G. Al-Sahlan, and M. Al-Awadhi. Quest of carbonate stringers in southwest kuwait using post stack seismic inversion technique. 2014(1):1–5, 2014. ISSN 2214-4609. doi: https://doi.org/10.3997/2214-4609.20141537. URL https://www.earthdoc.org/content/papers/10.3997/2214-4609.20141537.

[22] A.-S. M. Jasem, A.-E. Dakhil, and R. Arun. Drilling fluids challenges in successful drilling of gotnia formation in the state of kuwait. *International Petroleum Technology Conference*, 2013. doi: https://doi.org/10.2523/IPTC-16409-MS.

Appendix A

Parameter optimization remaining results

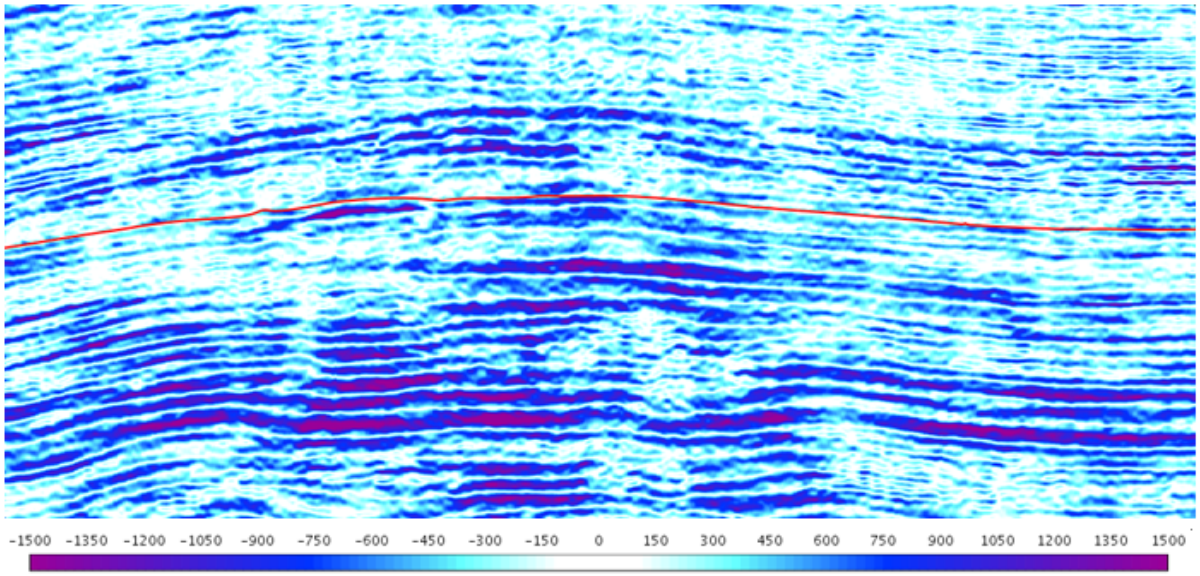

Figure A.1: 2nd parametrization residual xline cross-section of the target area (1800ms - 2800ms), performed by subtracting the results of one inversion from the other (sequential - joint).

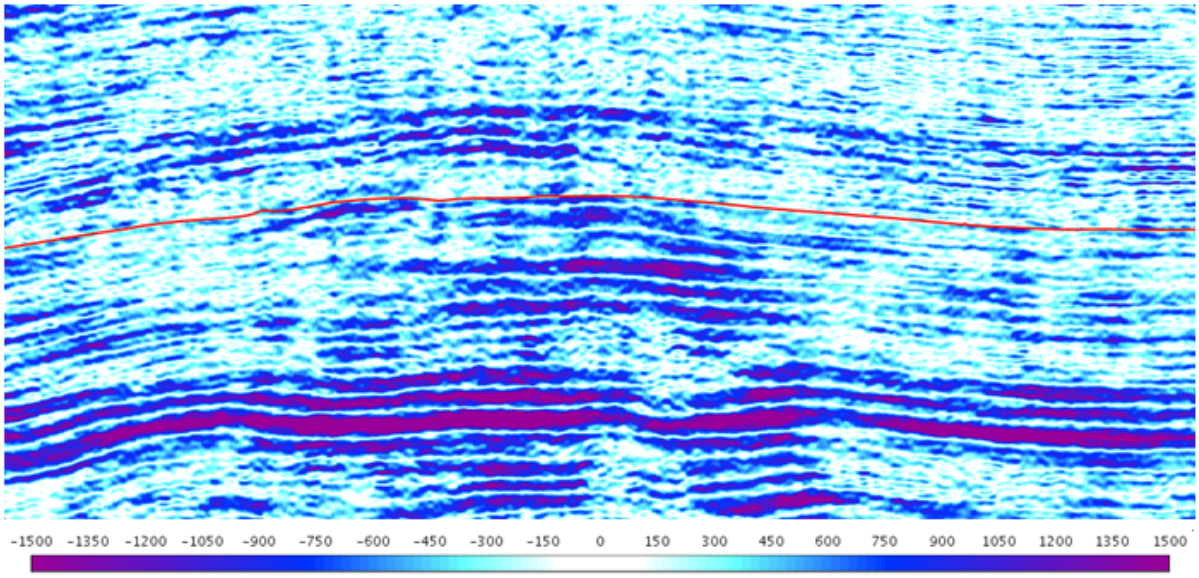

Figure A.2: 3rd parametrization residual xline cross-section of the target area (1800ms - 2800ms), performed by subtracting the results of one inversion from the other (sequential - joint).

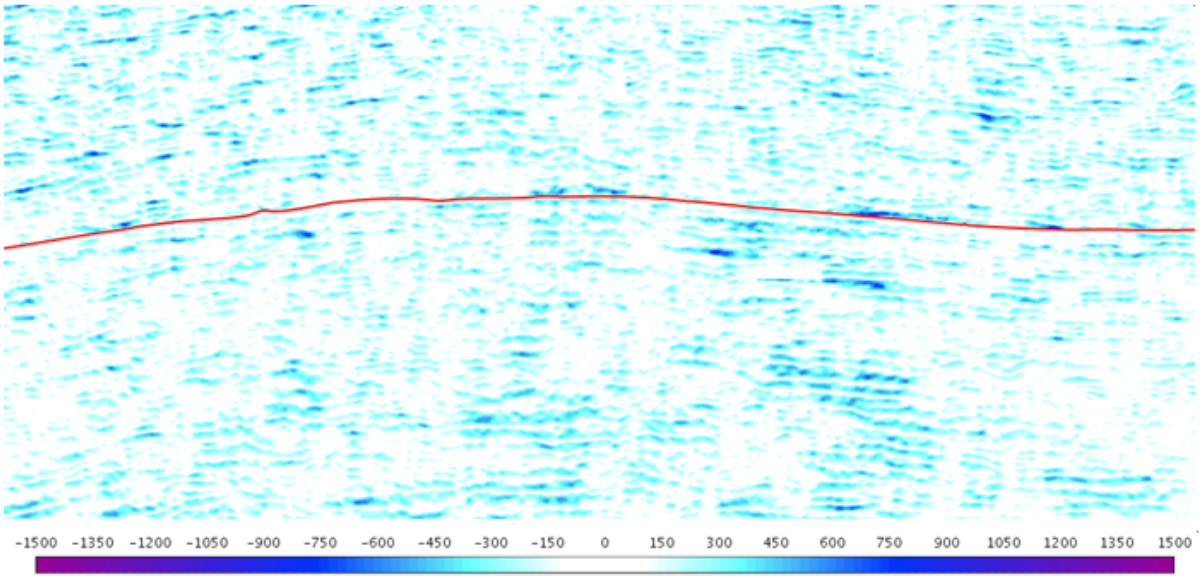

Figure A.3: 8th parametrization residual xline cross-section of the target area (1800ms - 2800ms), performed by subtracting the results of one inversion from the other (sequential - joint).

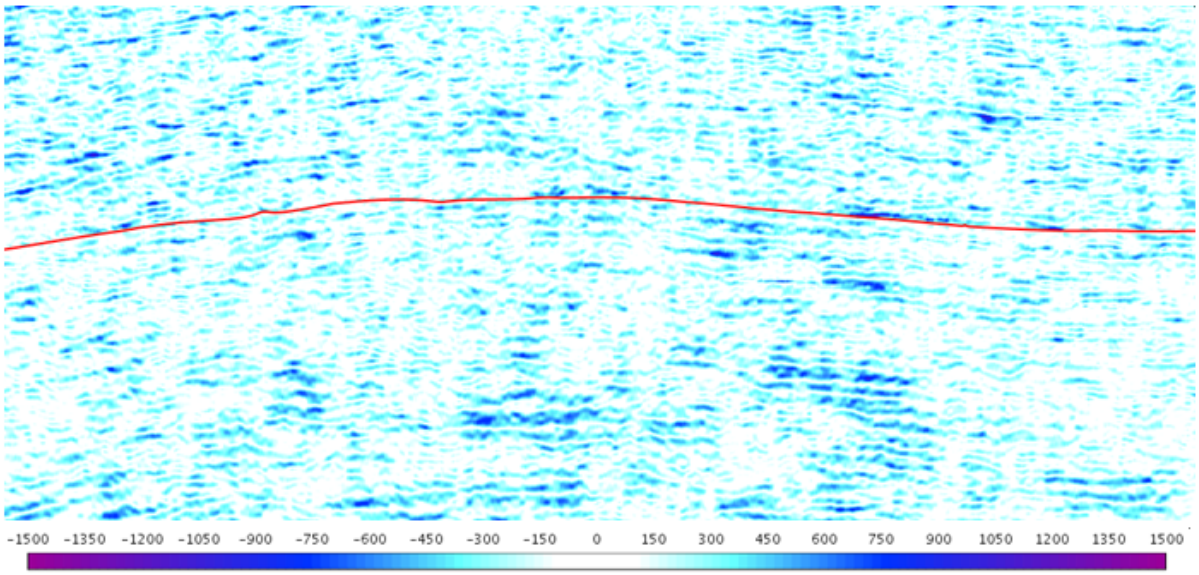

Figure A.4: 10th parametrization residual xline cross-section of the target area (1800ms - 2800ms), performed by subtracting the results of one inversion from the other (sequential - joint).

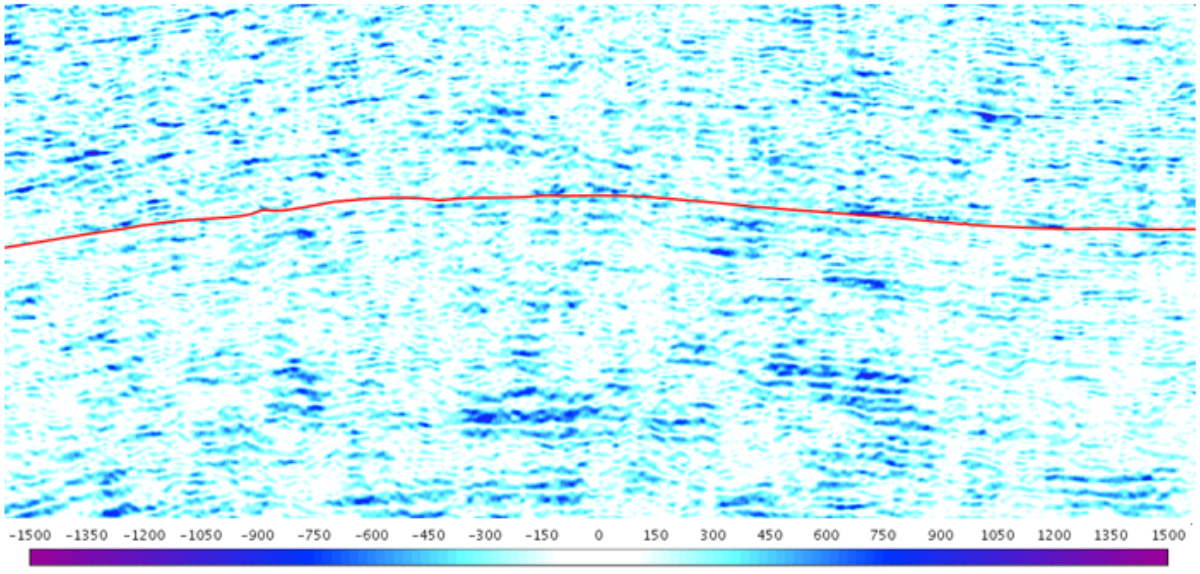

Figure A.5: 11th parametrization residual xline cross-section of the target area (1800ms - 2800ms), performed by subtracting the results of one inversion from the other (sequential - joint).

ISD Ratio (Sequential/Joint)	Parametrization	Inversion	ISD	Seismic N/S	Cost Function	Cost Function difference
1	1	Sequential	400	10	44,26%	25,80%
		Joint	400	10	70,06%	
	2	Sequential	800	10	70,27%	13,65%
		Joint	800	10	83,92%	
	3	Sequential	1200	10	80,74%	7,24%
		Joint	1200	10	87,98%	
0,67	4	Sequential	800	10	70,27%	17,71%
		Joint	1200	10	87,98%	
0,5	5	Sequential	400	10	44,26%	39,66%
		Joint	800	10	83,92%	
1,3	6	Sequential	1600	10	85,91%	2,07%
		Joint	1200	10	87,98%	
1,5	7	Sequential	1200	10	80,74%	3,18%
		Joint	800	10	83,92%	
2	8	Sequential	1000	10	76,53%	0,82%
		Joint	500	10	75,71%	
	9	Sequential	1200	10	80,74%	1,30%
		Joint	600	10	79,44%	
	10	Sequential	1400	10	83,72%	0,88%
		Joint	700	10	82,84%	
	11	Sequential	1600	10	85,91%	1,99%
		Joint	800	10	83,92%	
3	12	Sequential	1200	10	80,74%	10,68%
		Joint	400	10	70,06%	
4	13	Sequential	1600	10	85,91%	15,85%
		Joint	400	10	70,06%	

Figure A.6: Full parametrization inversion settings